INSTITUTO DE QUÍMICA

PROGRAMA DE PÓS-GRADUAÇÃO EM GEOCIÊNCIAS – GEOQUÍMICA

CAIO CÉZAR DE SOUZA GONÇALVES

MILLENNIAL-SCALE CHANGES IN BOTTOM-WATER OXYGENATION IN THE WESTERN EQUATORIAL ATLANTIC OVER THE LAST GLACIAL PERIOD

NITERÓI

2019

CAIO CÉZAR DE SOUZA GONÇALVES

MILLENNIAL-SCALE CHANGES IN BOTTOM-WATER OXYGENATION IN THE WESTERN EQUATORIAL ATLANTIC OVER THE LAST GLACIAL PERIOD

Dissertação apresentada ao Curso de Pós-Graduação em Geociências da Universidade Federal Fluminense, como requisito parcial para a obtenção do **Grau de Mestre**. Área de Concentração: **Geoquímica Ambiental**.

Orientadora:
Profª Drª Ana Luiza Spadano Albuquerque

Coorientadora:
Drª Bruna Borba Dias

NITERÓI
2019

Ficha catalográfica automática - SDC/BGQ
Gerada com informações fornecidas pelo autor

G635m Gonçalves, Caio Cézar de Souza
Millennial-scale changes in bottom-water oxygenation in the western equatorial Atlantic over the last glacial period / Caio Cézar de Souza Gonçalves ; Ana Luiza Spadano Albuquerque, orientadora ; Bruna Borba Dias, coorientadora. Niterói, 2019.
71 f. : il.

Dissertação (mestrado)-Universidade Federal Fluminense, Niterói, 2019.

DOI: http://dx.doi.org/10.22409/PPG-Geo.2019.m.14661790740

1. Foraminífero. 2. Isótopo estável de carbono. 3. Produção intelectual. I. Albuquerque, Ana Luiza Spadano, orientadora. II. Dias, Bruna Borba, coorientadora. III. Universidade Federal Fluminense. Instituto de Química. IV. Título.

CDD -

Bibliotecária responsável: Catia Vasconcellos Marques - CRB7/5116

CAIO CEZAR DE SOUZA GONÇALVES

MILLENNIAL-SCALE CHANGES IN BOTTOM-WATER OXYGENATION IN THE WESTERN EQUATORIAL ATLANTIC OVER THE LAST GLACIAL PERIOD

Dissertação apresentada ao Curso de Pós - Graduação em Geociências da Universidade Federal Fluminense, como requisito parcial para a obtenção do **Grau de Mestre**. Área de Concentração: **Geoquímica Ambiental**.

Aprovada em Fevereiro de 2019.

BANCA EXAMINADORA

PROFa. DRa. ANA LUIZA SPADANO ALBUQUERQUE
ORIENTADORA/UFF

PROFa. DRa. BRUNA BORBA DIAS
COORIENTADORA/UFF

PROFa. DRa. RUT AMELIA DIAZ RAMOS/UFF

PROF. DR. CRISTIANO MAZUR CHIESSI/USP

PROF. DR. NICOLAS MISAILIDIS STRIKIS
UFF

NITERÓI
2019

DEDICATION

I dedicate this work to all those who will take it into their hands,
whether by curiosity or search for knowledge.

ACKNOWLEDGEMENTS

I thank my parents who, first of all, are my heroes. Thank you for all the support and the continuous encouragement to fight for my dreams, and for never letting me succumb to adversity. The support received from you was and is the key of my success. Love you both!

I thank my sister for her complicity and friendship and for our many laughs in moments of joy. Finally, this little bratty has grown!

I thank my two supervisors Ana and Bruna for all their dedication, commitment and help in carrying out this work. Thank you for knowing the right time to demand and encourage. Without you, the path would have been much more arduous.

I thank the team of the Laboratório de Oceanografia Operacional e Paleoceanografia (LOOP) for becoming part of my family. And family that plays together, stays together.

I thank the professors and staff of the Departamento de Geoquímica for all knowledge acquired. You have helped me to become the professional I am today.

I thank my friends from the 2017.1 class for all the moments we spent together. With you, I started this walk, and with you, I am finishing it. We are always together!

I thank my friends from other classes in this department. Thanks for all the incredible moments, I will take them forever with me!

I thank my friends from Volta Redonda, who probably will never read this text, but who deserve to be remembered for all the attention, advice and support dedicated to me at this important stage of my life.

I thank CNPq and CAPES for granting the scholarship over the period of this master's degree.

Finally, I thank God for giving me the possibility of thanking!

EPIGRAPH

"*The fact that we live*
at the bottom of a deep gravity well,
on the surface of a gas covered planet
going around a nuclear fireball
90 million miles away
and think this to be normal
is obviously some indication
of how skewed our perspective
tends to be."

— Douglas Adams,
The Salmon of Doubt: Hitchhiking the Galaxy One Last Time

RESUMO

As mudanças ocorridas na circulação oceânica global influenciam diferentes processos que são determinantes para modificar a concentração de oxigênio em profundidades médias do Oceano Atlântico. Embora exista certo consenso sobre o que poderia levar a tais modificações (como as mudanças da circulação de fundo ou a produtividade exportada), o(s) mecanismo(s) preciso(s), especialmente na parte ocidental do Atlântico equatorial, permanecem sem uma explicação concreta. De forma a explorar os potenciais mecanismos em maior detalhamento, o presente trabalho teve como finalidade analisar o gradiente entre os isótopos estáveis de carbono de duas espécies de foraminíferos bentônicos (*Cibicides wuellerstorfi* e *Globobulimina affinis*) do Atlântico Equatorial Oeste para reconstruir, em escala milenar, mudanças na oxigenação de águas de fundo ao longo do último período glacial. Os dados mostraram que as diminuições mais significativas na concentração de oxigênio ocorreram durante os eventos denominados *Heinrich Stadials* (HS) (especialmente HS3, HS4 e HS5) como resultado da menor ventilação da Água Profunda do Atlântico Norte (do inglês, *North Atlantic Deep Water* – NADW), registrada por valores de $\delta^{13}C$ mais empobrecidos nas testas da espécie epifaunal *C. wuellerstorfi*. Além disso, os dados se mostraram consideravelmente relacionados com reduções na intensidade das correntes de fundo durante esses eventos, sendo representadas pela diminuição do tamanho da fração granulométrica '*sortable silt*' ($\overline{SS}$) que, por sua vez, favoreceu a deposição e acúmulo de matéria orgânica nos sedimentos. O presente trabalho também mostrou que os maiores valores de carbono orgânico total (COT) observados no testemunho GL-1248 não são provenientes da produtividade primária em superfície, mas sim do aporte continental através do Rio Parnaíba. Além disso, os maiores valores de COT se mostraram inconsistentes com o gradiente isotópico entre duas espécies de foraminíferos bentônicos (*Uvigerina peregrina* e *Cibicides wuellerstorfi*) que refletem o baixo fluxo de carbono orgânico lábil nos sedimentos. Consequentemente, a deposição e o acúmulo de matéria orgânica terrígena evitaram a difusão de O_2 nos sedimentos, desempenhando um papel fundamental nas mudanças de oxigenação no Atlântico Equatorial Oeste durante os HS ao longo da última deglaciação.

Palavras-chave: Foraminíferos. Isótopos estáveis de carbono. Oxigenação das águas de fundo. Ventilação da NADW. Atlântico Equatorial Oeste. Estadiais *Heinrich.*

ABSTRACT

Modifications in global ocean circulation influence many distinctive processes that drive changes in the oxygen concentration in the Atlantic mid-depths. Although there is some consensus about what could lead to these changes (such as the bottom circulation or export of primary productivity), the precise mechanism(s), especially in the western equatorial Atlantic, remain unexplained. To explore potential mechanisms in more detail, the present work aimed to analyze the gradient between the stable carbon isotopic records of two benthic foraminifera species (*Cibicides wuellerstorfi* and *Globobulimina affinis*) from the western equatorial Atlantic (WEA) to reconstruct millennial-scale changes in the bottom-water oxygenation over the last glacial period. The records demonstrated that the most prominent decreases in oxygen concentration occurred during the Heinrich Stadial (HS) events (especially HS3, HS4 and HS5) as a result of lower North Atlantic Deep Water (NADW) ventilation, indicated by more depleted $\delta^{13}C$ values in the epifaunal *C. wuellerstorfi*. Furthermore, the results were consistently related to decreases in the strength of the bottom-water currents during these events, reflected by the decrease of the 'sortable silt' grain-size fraction ($\overline{SS}$), which favored the deposition and accumulation of organic matter in the sediment. The present work also showed that the highest values of total organic carbon (TOC) at GL-1248 site are not derived from surface primary productivity, but rather from continental input via the Parnaíba River. Moreover, the higher TOC values were inconsistent with the isotopic gradient between two benthic foraminifera species (*Uvigerina peregrina* and *Cibicides wuellerstorfi*) that reflect the low flux of labile organic carbon in the sediments. Consequently, the deposition and accumulation of terrigenous organic matter avoided the diffusion of O_2 into the sediments, playing an important role in the oxygen concentration changes in the WEA during the HS over the last deglaciation.

Keywords: Foraminifera. Stable carbon isotopes. Bottom-water oxygenation. NADW ventilation. Western Equatorial Atlantic. Heinrich Stadials.

LIST OF FIGURES

LIST OF TABLES

NOMENCLATURE

AABW	Antarctic Bottom Water
AAIW	Antarctic Intermediate Water
AMOC	Atlantic Meridional Overturning Circulation
CDW	Circumpolar Deep Water
CO_2	Carbon dioxide
DIC	Dissolved Inorganic Carbon
DWBC	Deep Western Boundary Current
EUC	Equatorial Undercurrent
HS	Heinrich Stadial
ITCZ	Intertropical Convergence Zone
LGM	Last Glacial Maximum
NADW	North Atlantic Deep Water
NBC	Northern Brazil Current
NECC	North-Equatorial Countercurrent
NEUC	North-Equatorial Undercurrent
O_2	Oxygen
SACW	South Atlantic Central Water
SEC	South-Equatorial Current
Sv	Sverdrups
TOC	Total Organic Carbon
TROX	TRophic conditions and OXygen concentrations
TW	Tropical Water
VPDB	Vienna Pee Dee Belemnite
WEA	Western Equatorial Atlantic
$\delta^{13}C$	Stable carbon isotope ratio ($^{13}C/^{12}C$)
$\delta^{18}O$	Stable oxygen isotope ratio ($^{18}O/^{16}O$)
$\overline{SS}$	Sortable Silt
$[O_2]$	Oxygen concentration
$\Delta\delta^{13}C$	Gradient between stable carbon isotopes

SUMMARY

1 INTRODUCTION

The oceans strongly influence Earth's climate since they constitute one of the largest stocks of the carbon cycle. Ocean-atmosphere interactions control the heat and carbon dioxide (CO_2) exchange between those compartments, which is decisive for global climate variability. In the Atlantic Ocean, these interactions are strongly modulated by changes in the Atlantic Meridional Overturning Circulation (AMOC), which influences the climate on glacial-interglacial timescales due to the ocean's thermal capacity to regulate heat transport on its surface and the efficient storage and release of CO_2 in the deep ocean (ADKINS, 2013; BROECKER, 1982; DENTON et al., 2010). On millennial timescales, Heinrich Stadial (HS) are defined as periods that represent the most prominent changes in AMOC transport, when the formation of the North Atlantic Deep Water (NADW) was probably not completely ceased (MCMANUS et al., 2004), but was at least significantly reduced (BRADTMILLER; MCMANUS; ROBINSON, 2014; GHERARDI et al., 2005; OPPO; CURRY; MCMANUS, 2015). Those events are characterized by cold conditions in the Northern Hemisphere, during which a large amount of fresh water reached the regions of deep-water formation due to massive iceberg rafting into the North Atlantic (BOND et al., 1992; HEINRICH, 1988; HEMMING, 2004). The modification of the deep ocean circulation during these events promotes the alteration of large-scale patterns of nutrient outcropping, which imposes significant biological consequences related to the production and consumption of organic carbon, either labile or respired. This pattern contributes substantially to increases or decreases in atmospheric CO_2 (MENVIEL et al., 2018; SIGMAN; BOYLE, 2000; TOGGWEILER; RUSSELL; CARSON, 2006) as a result of large-scale modifications in bottom-water oxygenation, such as the expansion and retraction in the extent of the oxygen minimum zones (KOHO; DE NOOIJER; REICHART, 2015).

Modifications in the deep ocean circulation are strictly related to changes in bottom-water properties (such as temperature, salinity, density, pH and nutrient content) and, because of its importance in regulating organic carbon cycling (DAUWE; MIDDELBURG; HERMAN, 2001; HEDGES; KEIL, 1995), reconstructions of bottom-water oxygenation are crucial for evaluating the amount of respired carbon stored at mid-depths. Depleted stable carbon isotope ($\delta^{13}C$) values in benthic foraminifera in the deep Atlantic during the last glacial period provide, for example, evidence for reduced ventilation during cold stadials (BURCKEL et al., 2015; SCHMITTNER;

LUND, 2015; VOIGT et al., 2017) and point to decreased deep-water oxygen concentration ($[O_2]$) due to O_2 consumption via microbial respiration. Hoogakker; Thornalley & Barker (2016) suggested that the $[O_2]$ in the deep North Atlantic was 45 and 65 $\mu mol.kg^{-1}$ lower during the penultimate and last glacial periods relative to present values and that the concentration of remineralized organic carbon was twice as high during the glacial maxima as they are currently. Indeed, decreased ventilation linked to a reorganization of ocean circulation (i.e. the way the oceans can return to their original characteristics) is thought to be a primary cause for those changes in oxygen concentration (GOTTSCHALK et al., 2016a), especially when accompanied by a strengthened global biological pump (KOHFELD et al., 2005).

Changes in bottom-water oxygenation can be reconstructed from carbon isotope gradients between bottom-water and pore water signals (HOOGAKKER et al., 2015; MCCORKLE; EMERSON, 1988). The $[O_2]$ in sediment pore water reflects the balance between consumption and diffusion (EMERSON et al., 1985), which is depleted at the anoxic boundary, where the $[O_2]$ is zero. Hence, the total amount of remineralized organic carbon depends on the bottom-water $[O_2]$, such that the more organic matter is remineralized, the more isotopically light is the $\delta^{13}C$ signal that releases in pore waters (HOOGAKKER et al., 2015). If the $\delta^{13}C$ signal of an epifaunal foraminiferal species reflects the bottom-water signal and if the $\delta^{13}C$ signal of a deep infaunal foraminiferal species reflects the pore water signal (MCCORKLE; EMERSON, 1988), then the $\delta^{13}C$ gradient between these two species can be used to reconstruct the bottom-water $[O_2]$ (GOTTSCHALK et al., 2016a; HOOGAKKER et al., 2015; HOOGAKKER; THORNALLEY; BARKER, 2016).

Previous studies have proposed that changes in the bottom-water oxygen content have been related to variations in the amount of respired carbon stored in the deep Atlantic (HOWE et al., 2016; VOIGT et al., 2017), rather than to differences in water mass mixing and/or sources of formation in the North Atlantic (CURRY; OPPO, 2005; LUND et al., 2015), particularly during HS. The majority of such studies are based on the northern portion of the Atlantic (HOOGAKKER et al., 2015; HOOGAKKER; THORNALLEY; BARKER, 2016) and the Southern Ocean (GOTTSCHALK et al., 2016a; JACCARD et al., 2016); however, there are no studies that approach the millennial-scale reconstruction of bottom-water oxygenation in the western equatorial Atlantic (WEA) margin over the last glacial period.

Faced with this gap, this study was proposed as a way to investigate the underlying causes for millennial-scale decreases in stable carbon isotopic anomaly in benthic foraminifera in the mid-depth (2,264 m) equatorial Atlantic, as well as report millennial-scale bottom-water [O_2] reconstructions for the WEA from the core GL-1248, whose location was influenced by the Deep Western Boundary Current (DWBC) that carries the NADW at mid-depths.

In order to better understand the approach of this work, it was created a simplified conceptual model (Figure 1) that synthesize the main processes that influence the bottom-waters dynamics during the glacial and HS at mid-depths in the WEA.

Figure 1 – Conceptual model that resume the expected changes in bottom-water circulation and bottom-oxygenation during (A) the glacial period and (B) the HS at mid-depths in the WEA (both related to the interglacial period). The different sizes of vertical arrows (in purple) indicate the amount of organic material exported in the water column and in the sediments. The different sizes of the horizontal arrows (in green) indicate the intensity of the circulation of the bottom-waters. Blue and red arrows indicate the intensity of the increase or the decrease of the parameters analyzed. In the case of both $\Delta\delta^{13}C$, the arrows indicate bigger (↑) or smaller (↓) gradient between the species. Epifaunal stands for *Cibicides wuellerstorfi*, shallow infaunal stands for *Uvigerina peregrina* and deep infaunal stands for *Globobulimina affinis*

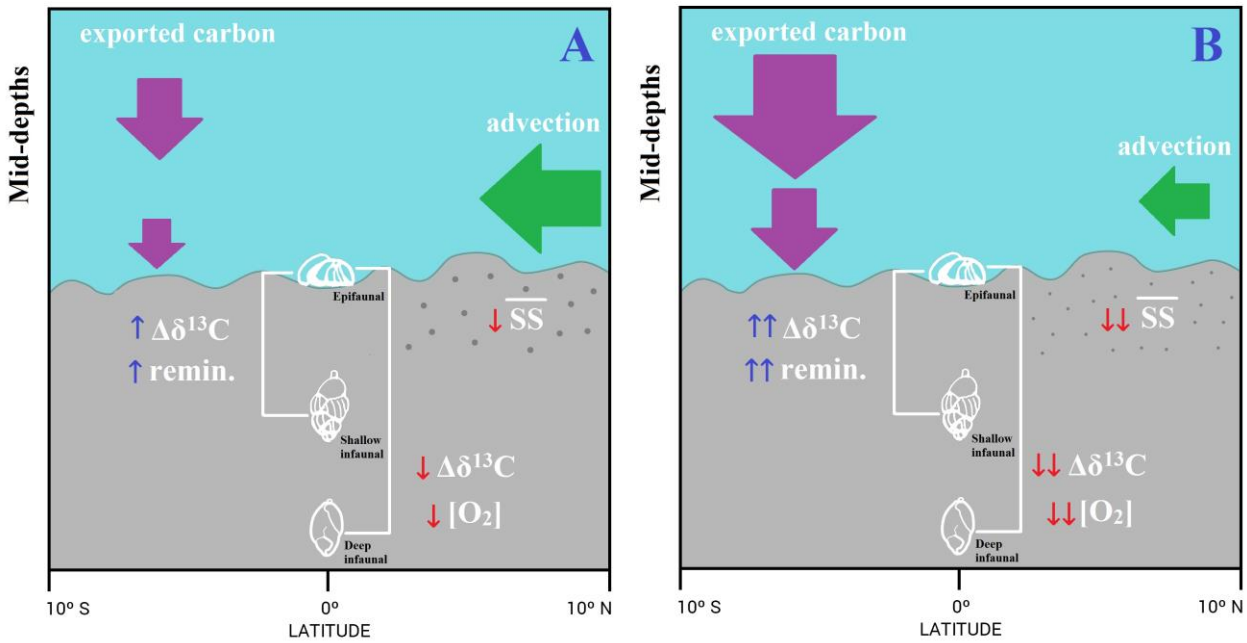

Source: GONÇALVES, 2019.

During the glacial (Figure 1A), the advection of the NADW partially prevents the exported carbon flux in the bottom-waters as a consequence of the return of the AMOC circulation, which are reflected by the not so low values of $\overline{SS}$ mean size. In this way, the carbon

remineralization is significant, but not expressive, resulting in an increase in the gradient ($\Delta\delta^{13}C$) between the shallow infaunal foraminifera (*Uvigerina peregrina*) and the epifaunal foraminifera (*Cibicides wuellerstorfi*). Hence, the oxygen concentration is a little reduced when compared to the interglacial period, as indicated by the decrease in the gradient ($\Delta\delta^{13}C$) between the epifaunal foraminifera (*Cibicides wuellerstorfi*) and the deep infaunal foraminifera (*Globobulimina affinis*).

During the HS (Figure 1B), the reduced advection of the NADW contributes to the increase of the exported carbon in the bottom-waters, so a large amount of carbon is settled in the sediments due to the weak advective transport of the NADW and the deceleration of the AMOC, which are reflected by the lowest values of $\overline{SS}$ mean size. In this scenario, the carbon remineralization is very significant, resulting in a bigger gradient ($\Delta\delta^{13}C$) between the shallow infaunal foraminifera (*Uvigerina peregrina*) and the epifaunal foraminifera (*Cibicides wuellerstorfi*). As a consequence of the remineralization process that consumes organic matter, the oxygen concentration is significantly reduced as indicated by the smaller gradient ($\Delta\delta^{13}C$) between the epifaunal foraminifera (*Cibicides wuellerstorfi*) and the deep infaunal foraminifera (*Globobulimina affinis*).

Based on the introduction and the proposed conceptual model, the following hypotheses were tested in this study:

***HYPOTHESIS 1*:** The $\delta^{13}C$ signal of the epifaunal foraminifera (*Cibicides wuellerstorfi*) from mid-depths does not record changes in the mixture of bottom-waters, but the reduced NADW ventilation observed during the last glacial.

***HYPOTHESIS 2*:** The flux of the bottom-waters in the WEA is related to the millennial-scale oscillations of the AMOC during the last glacial period, which, in turn, control the ventilation in mid-depths. The reduced ventilation caused by the reduced advection favors the deposition of terrigenous organic carbon from continent, preventing the diffusion of oxygen into the sediments and modifying the redox conditions of the environment.

2 OBJECTIVES

The general objective of this study is to reconstruct the bottom-water oxygenation in the WEA over the last glacial period in a millennial-scale oscillation, in order to verify how oxygen concentration is linked to the carbon cycle and the mid-depth circulation, as well as to understand the processes and mechanisms that control such changes by using geochemical and sedimentological analyzes (bulk) and micropaleontological and isotopic analyzes in foraminifera species.

2.1 SPECIFIC OBJECTIVES

The specific objectives proposed for the present study are:

- to use the stable carbon isotope ($\delta^{13}C$) of benthic foraminifera in order to understand the dynamics in the bottom-waters and ventilation of the Atlantic Ocean;
- use the geochemical analyzes of the sediment (i.e. total organic carbon) to elucidate its role in the diffusion of oxygen in the sediments;
- analyze the relative abundance of three productivity-related foraminifera species as indicator of surface primary productivity;
- verify the variation of the sediment grain size in order to identify the variability of the deposition processes and the dynamics of the bottom-water masses;
- use the Ti/Ca ratio as a proxy for continental input of terrigenous material;
- use the relationship between $\delta^{13}C$ signals of epifaunal (*Cibicides wuellerstorfi*) and deep infaunal (*Globobulimina affinis*) foraminifera species as a proxy of bottom-water oxygenation changes;
- use the relationship between $\delta^{13}C$ signals of epifaunal (*Cibicides wuellerstorfi*) and shallow infaunal (*Uvigerina peregrina*) foraminifera species as a proxy of organic matter fluxes;
- integrate all the variables in order to understand the relationships between the bottom-water masses, the carbon cycle and AMOC dynamics over the last glacial period.

3 THEORETICAL BASIS

3.1 FORAMINIFERA

The foraminifera (from Latin foramina = orifice, fera = to possess) are unicellular, eukaryotic and heterotrophic microorganisms, classified in the Eukarya Domain, Rhizaria Group, Foraminifera Phylum (BURKI, 2014). They are cosmopolitan and predominantly marine, with only one family of freshwater (Allogromiidae). They have an average size ranging from 100 μm to 1 mm, but may be bigger than that, such as the already extinct *Lepidocyclina elephantina* Lemoine and Douvillé, 1904, with 14 cm in size and the *Neusina agassizi* Goës, 1892, with 19 cm in size (BIGNOT, 1988; SEN GUPTA, 2003).

These microorganisms secrete a carapace, or test, which may be composed of calcareous material or constituted of agglutinated mineral and biogenic particles, but rarely of organic (Allogromiidae Family) or silicon composition (Silicoloculinidae Family). The group taxonomy is mainly based on the carapace wall composition and morphology, taking into account the shape, the types of apertures and chambers winding, and the presence or absence of external structures (ARENILLAS, 2004). Related to the carapace composition, these microorganisms can be divided into three principal types, as characterized below (CAMACHO; LONGOBUCCO, 2007):

a) agglutinated: the tests are composed of organic and mineral material from the sediment mixed with an organic, calcareous or ferrous oxide cement. The grains are selected by size, texture or composition. Species with this characteristic are included in the Textulariina Suborder.
b) porcelain: the tests are composed of small needles of randomly arranged calcite secreted by the organism. They have a uniform, impervious, smooth and homogeneous appearance, with a bright white surface. Species with this characteristic are included in the Miliolina Suborder.
c) hyaline: the tests are also composed of calcite secreted by the organism, but with a glassy or translucent appearance, generally presenting ornaments. Species with this characteristic are included in the Rotaliina, Spririliina, Involutinina and Robertinina Suborder.

The foraminifera carapace is divided into one or more chambers, small septa that divide the carapace internally, and foramen, which connects the inner chambers (CORLISS; CHEN, 1988; SEN GUPTA, 2003). Externally, these microorganisms have a cytoplasmic mass called ectoplasm that project through the pores, in the form of reticulated pseudopods, in the way that are used for locomotion, respiration, food capture, carapace construction and fixation (SEN GUPTA, 2003). They are omnivores and usually feed on bacteria, algae, diatoms, organic particles, invertebrate larvae and other protozoa (ARENILLAS, 2004; BOLTOVSKOY; 1965).

The foraminiferal organisms can have a benthic or planktonic habitat. The benthic ones were the first to appear in the fossil record at the beginning of the Cambrian period (545 Ma ago) as agglutinating forms, and later in the Silurian period (444 Ma ago) as calcareous forms. They live associated with the marine sediment, may present specific movements or be totally sessile by attaching themselves to the seafloor through the carbonate cementation (ARMSTRONG; BRASIER, 2005). Benthic foraminifera can have an epifaunal life habit, by living on the surface of the seafloor sediments, or infaunal life habit, by living buried in the first few centimeters of the sediment (Figure 2), using their cytoplasm projections or calcareous secretions to fix themselves (CORLISS; CHEN, 1988). The different life habitats of these benthic organisms are mainly related to specific food and oxygen demands that dictates where they live in the sediments (JORISSEN; DE STIGTER; WIDMARK, 1995). On the other hand, the planktonic organisms emerged just at the end of the Triassic period (205 Ma ago). They do not have their own locomotion movements. Instead, they inhabit the water column by floating passively, being dispersed under the current actions and controlled seasonally by lunar cycles (MOLINA, 2004).

Figure 2 – Representation of some typical benthic foraminifera species life habit position, living above the surface (epifaunal) and living within the sediments (infaunal)

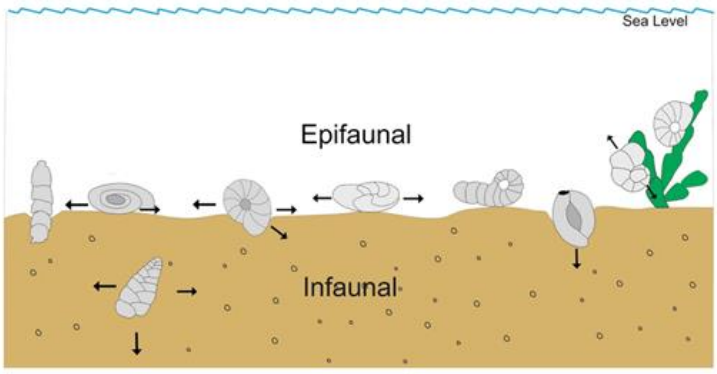

Source: CHAN et al., 2017.

3.2 BENTHIC FORAMINIFERA AND THEIR APPLICATION IN PALEOCEANOGRAPHIC STUDIES

The first mention of foraminifera was made by Herodotus (about 485-425 B.C.), who observed the presence of lenses format objects in the limestones of the Egyptian pyramids, nowadays known as the Genus Nummulites foraminifera. However, it took more than two hundred years after the first mention to be produced the first classification and recognition of these organisms in a work entitled "*Tableau méthodique de la classe des Céphalopodes*", by Alcide d'Orbigny. More recently, Joseph Cushman stands out as one of the first people to use the foraminifera as biostratigraphic indicators in order to determine seafloor sediments age (CUSHMAN, 1928).

The applicability of the foraminifera species in many different areas (e.g. petroleum exploration, biostratigraphy, paleoceanographic and paleoclimatic studies) mainly relies on the fact that they are present in all the oceans, have shells easily preserved in the marine sediments, have a rapid evolutionary development and have high diversity (CUSHMAN, 1928; LOEBLICH; TAPPAN, 1988). Over the years, studies have been carried out for paleobathymetric determinations, focused mainly on isobathic species that inhabit the same depth in all oceans (BANDY; ARNAL, 1957; PHLEGER; PARKER, 1951). Furthermore, it was proposed the calculation of the ratio between planktonic and benthic foraminifera as bathymetric determinants, still widely used nowadays, in addition to the ratio between the number of agglutinated, porcelain and hyaline shells as depth indicators (ARMSTRONG; BRASIER, 2005) (Figure 3).

Over time, many studies detailed the different physical-chemical features that can vary in the environment (such as sediment type, bathymetry, pH and salinity) and can have influence in the distribution of the benthic foraminifera across the oceans. In addition to pH and salinity, other parameters such as temperature and nutrient supply are responsible for promoting the development of specific fauna associations, suggesting changes in the influence of bottom-waters between glacial and interglacial periods (DESSANDIER et al., 2015; GOODAY, 1994; SCHMIEDL; MACKENSEN, 1997; STREETER, 1973). Others studies have begun to recognize specific communities living in poor-oxygenated environments (BERNHARD, 1986; SEN GUPTA; MACHAIN-CASTILLO, 1993; VAN DER ZWAAN, 1982; VENTURELLI et al., 2018), generally with low diversity and dominated by a few species adapted to develop under

limiting requirements. As a consequence, the oxygen concentration of deep waters has been gradually accepted as one of the most important environmental factors that globally influence benthic foraminifera fauna (BERNHARD, 1986; SEN GUPTA; MACHAIN-CASTILLO, 1993; VAN DER ZWAAN, 1982; VENTURELLI et al., 2018). When used as indicators of ocean productivity, the associations of the benthic foraminifera are mainly controlled by the addition of organic matter and the oxygenation of the bottom-waters, being more important than water depth, temperature, and salinity (BERGER; WEFER, 1990).

Figure 3 – Some typical planktonic and benthic foraminifera abundance and their changes with depth, latitude, and temperature

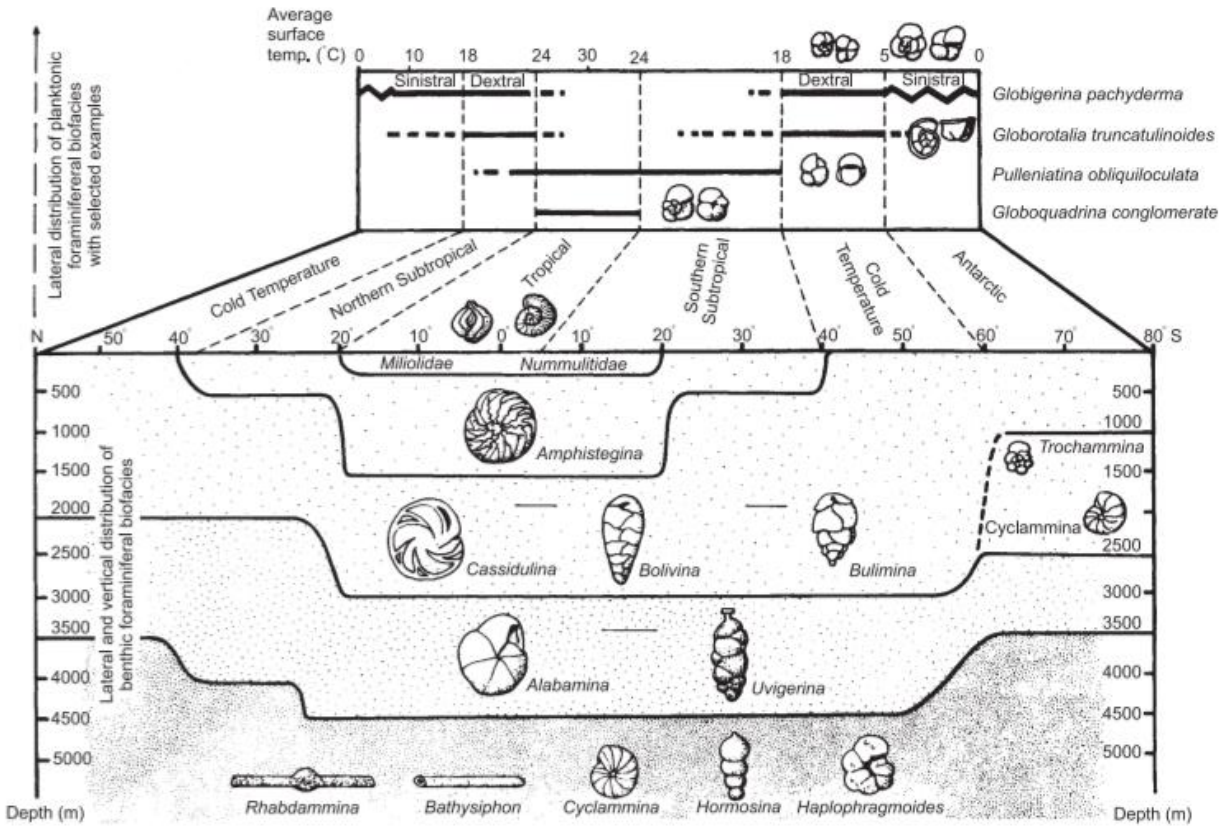

Source: ARMSTRONG; BRASIER, 2005.

Studies from Corliss (1985) and Corliss & Chen (1988) observed that benthic foraminifera can also inhabit the first ten centimeters of the ocean sediments, in environments that become increasingly poor in oxygen as they move down into the sediments. The epifaunal species inhabit the surface of the sediment, characterizing well-oxygenated habitats, while the

infaunal ones live buried in the sediment, being associated to environments of low oxygen concentration (CORLISS; CHEN, 1988).

In such approach, Jorissen; de Stigter & Widmark (1995) proposed the so-called TROX model (from TRophic conditions and OXygen concentrations) (Figure 4), which establishes that benthic organisms can live with a certain amount of oxygen availability. In addition, when oxygen is present, the vertical distribution of benthic foraminifera in the sediment is controlled by food availability. In oligotrophic environments, all organic matter is consumed on the surface of the sediment, resulting in the absence of infaunal species. In mesotrophic to eutrophic areas, a considerable increase in microhabitat depth is observed as a result of the consumption of the organic matter, which is no longer restricted to the surface sediments. The organic matter is led to deeper layers of the sediment (i.e. by bioturbations), where nutrients are supplied to the infaunal species. On the other hand, in very eutrophic habitats, the critical oxygen level created by the consumption of organic matter is bigger than the transport of it into the sediments, which limits the presence of the epifaunal species at the surface sediment layer (JORISSEN; DE STIGTER; WIDMARK, 1995).

Figure 4 – TROX model showing how oxygen concentration and food availability influence the limits of benthic foraminifera microhabitats in the sediments

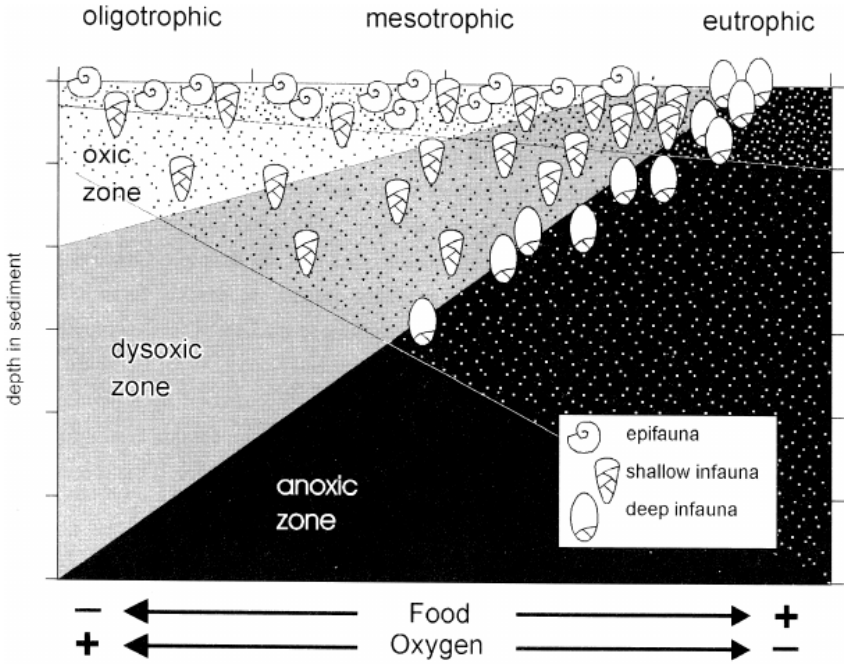

Source: JORISSEN; DE STIGTER; WIDMARK, 1995.

3.3 STABLE CARBON ISOTOPES ($\delta^{13}C$) IN BENTHIC FORAMINIFERA

The use of stable isotopes has become an essential part of marine geochemistry, contributing significantly to the understanding of past and present environmental changes of the oceans (HOEFS, 2009). In some areas, such as paleoclimatology and paleoceanography, there are many applications of stable isotopes in order to understand the climatic changes and the processes involved on it (ADKINS, 2002; HONISCH et al., 2009; WANG; TIAN; LOURENS, 2010). In this aspect, among other main elements, stands out the stable isotopes of carbon, one of the most abundant elements in the land.

Carbon has atomic number 6 and atomic mass 12. It presents two stable isotopes (^{12}C and ^{13}C) and four unstable isotopes (^{10}C, ^{11}C, ^{14}C, and ^{15}C). Their stable isotopes occur in the following proportion: ^{12}C = 98.89% (6 protons and 6 neutrons) and ^{13}C = 1.11% (6 protons and 7 neutrons) (RAVELO; HILLAIRE-MARCEL, 2007).

The carbon isotopic fractionation in calcite foraminifera is primarily controlled by the fractionation of dissolved inorganic carbon (DIC) in seawater, which is primarily dependent on the activity of primary productivity in the photic layer (very variable) and the global deep-sea carbon reservoir (stable for thousands of years). The last one, in turn, depends on carbon sources for the ocean (chemical weathering of continental rocks and hydrothermal activity), which are determinants for the global carbon cycle (KATZ et al., 2010) (Figure 5).

Figure 5 – Scheme showing photosynthesis (on land and in the surface ocean) acting in the carbon isotope fractionation by converting inorganic carbon to organic form and causing large negative shifts in $\delta^{13}C$ values of the organic carbon produced

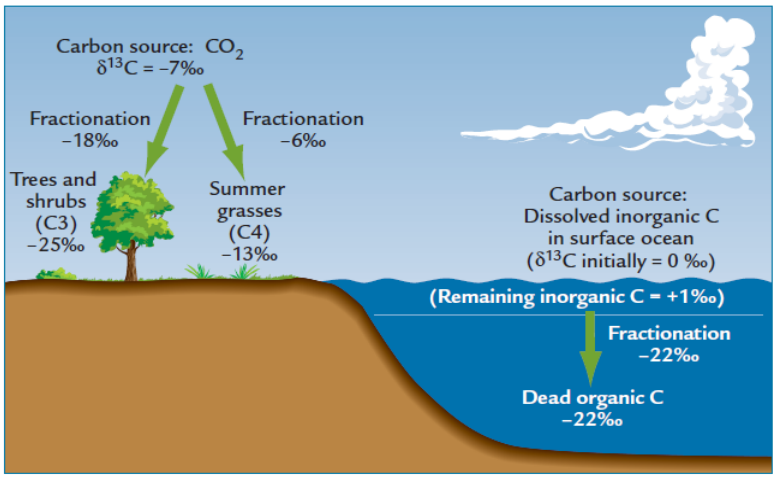

Source: RUDDIMAN, 2008.

The delta signal ($\delta^{13}C$) represents the deviation of the the ratio between the two stable isotopes (^{12}C and ^{13}C) that is measured in the calcite foraminifera by following the formula (KATZ et al., 2010):

$$\delta^{13}C_{sample} = \{[(^{13}C/^{12}C)_{sample} - (^{13}C/^{12}C)_{standard}] / (^{13}C/^{12}C)_{standard}\} \times 1000$$

The calibration of $\delta^{13}C$ analyzes on calcite foraminifera is done using the VPDB (for Vienna Pee Dee Belemnite) standard, based on belemminite fossils (Belemnitella americana) from the Cretaceous (RAVELO; HILLAIRE-MARCEL, 2007) and the values are expressed per-mille (‰). For convention, more positive $\delta^{13}C$ values have relatively large amounts of ^{13}C compared with ^{12}C and are referred to as ^{13}C-enriched or ^{12}C-depleted. Reversely, more negative $\delta^{13}C$ values have relatively small amounts of ^{13}C compared with ^{12}C and are referred to as ^{13}C-depleted or ^{12}C-enriched (RUDDIMAN, 2008).

However, it must be careful when analyzing the variations in the $\delta^{13}C$ of benthic foraminifera, since the fractionation in these species can be caused by environmental effects, such as microhabitat changes of the species (CORLISS, 1985; TACHIKAWA; ELDERFIELD, 2002), variations in the carbonate system (SPERO et al., 1997), CO_2 exchange between the ocean and atmosphere (PIOTROWSKI et al., 2008), and exported productivity.

The relationship between the $\delta^{13}C$ of the DIC and the primary productivity relies on the fact that producing organisms prefer to assimilate ^{12}C molecules (more labile), resulting in a depletion of ^{13}C in the organic matter and an enrichment in the surrounding water (MASLIN; SWANN, 2006). The $\delta^{13}C_{DIC}$ is variable over time and its fractionation may respond to changes in the circulation of deep-waters or to variations in productivity, with ^{12}C exported from the surface to the bottom seafloor. After the assimilation of ^{12}C by phytoplankton organisms, they are respired in the bottom-waters and/or deposited in the sediment, where the oxidation process of the organic material releases nutrients and CO_2 with depleted ^{13}C to the bottom and porewaters (KATZ et al., 2010) (Figure 6).

Figure 6 – Simplified scheme showing the sequence of events that makes possible the interpretation of the carbon isotopic fractionation from primary productivity variations

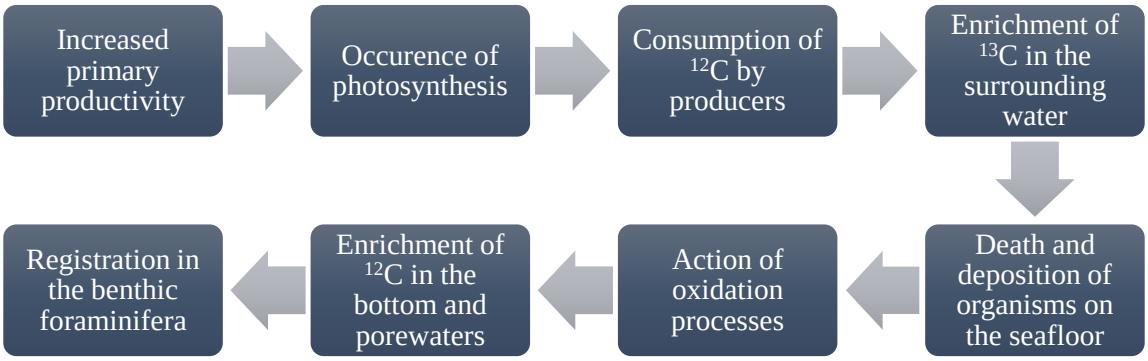

Source: GONÇALVES, 2019.

The isotopic difference between benthic foraminiferal species is generally attributed to habitat differences, the presence of symbionts and vital effect. In terms of different habitats, the chemistry of pore waters differs from the bottom-water because of the remineralization process that consumes organic matter, which changes the chemical composition into the sediments. Once the carbon isotopes are very sensitive to organic matter oxidation in the sediments, the $\delta^{13}C_{DIC}$ of the pore water, in this case, is considerably reduced. Thus, the $\delta^{13}C_{DIC}$ profile of the pore water tends to decrease with increasing of sediments depth. Epifaunal species, such as *Cibicides wuellerstorfi*, suffer the influence of bottom-waters, while shallow and deep infaunal species, such as *Uvigerina peregrina* and *Globobulimina affinis*, respectively, are influenced by pore waters. The gradient between $\delta^{13}C$ values of epifaunal and infaunal species may reflect the degree of preservation of the organic material in the sediment. When the difference between shallow infaunal and epifaunal species is close to 0‰, it indicates low organic contribution on the surface and in the sediments (KATZ et al., 2010; MACKENSEN et al., 2017; MCCORKLE et al., 1990; THEODOR et al., 2016). Furthermore, when the gradient between epifaunal and deep infaunal species gets closer to 0‰, it indicates anoxic conditions in the sediments (HOOGAKKER et al., 2015; MCCORKLE; EMERSON, 1988). Here, it is important to emphasize that the $\Delta\delta^{13}C$ gradient is inversely read in respect to shallow and deep infaunal species.

3.4 DIFFERENT PATTERNS OF OCEAN CIRCULATION IN THE ATLANTIC

The global ocean circulation pattern can be represented by a layer scheme that illustrates the various levels of water masses present in the water column. Each layer has very specific characteristics, which make them distinguishable from each other. These characteristics are intrinsically linked to the climatic events of the places where they were formed, so that they affect their temperature and salinity (MARSHAK, 2013).

The combination of these two parameters (temperature and salinity) determines the density of the water mass and its location along the water column (Figure 7). In this way, the bottom circulation pattern of the Atlantic Ocean is controlled by the ocean floor topography and by the distribution of the denser water masses, while the surface circulation pattern is governed by two large gyres driven by the trade winds in the equatorial region (counterclockwise direction to the South Atlantic and clockwise to the North Atlantic).

Figure 7 – Illustrative chart showing a simplified view of the stratification of different water masses located in the Atlantic Ocean driven by density variations

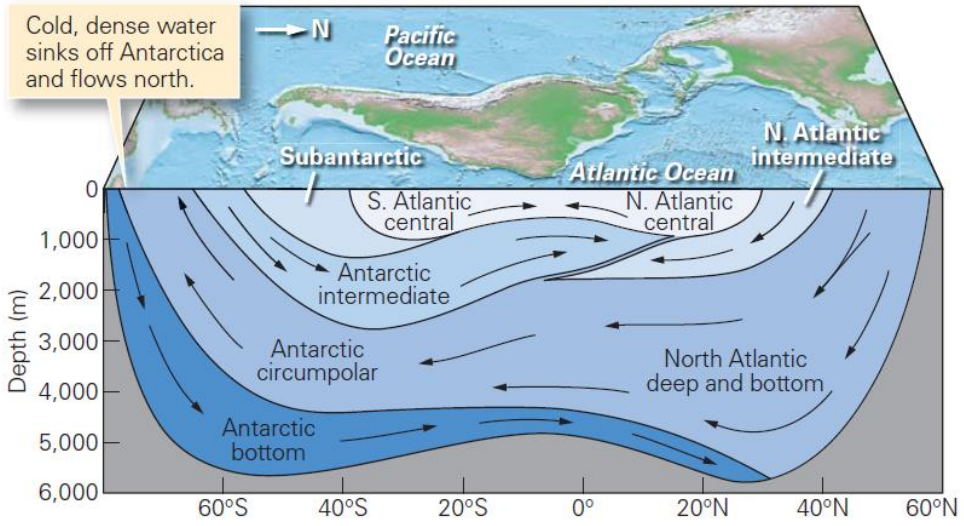

Source: MARSHAK, 2013.

According to Stramma & England (1999), the circulation pattern in the South Atlantic encompasses the following water masses: Tropical Water (TW), South Atlantic Central Water (SACW), Antarctic Intermediate Water (AAIW), Circumpolar Deep Water (CDW), North Atlantic Deep Water (NADW), and Antarctic Bottom Water (AABW) (Table 1).

Table 1 – Temperature and salinity values from water masses present in the South Atlantic

Water Mass	Acronyms	Thickness (m)	Temperature (ºC)	Salinity (µm.kg^{-1})
Tropical Water	TW	0 – 142	> 20	> 36.20
South Atlantic Central Water	SACW	142 – 567	20 – 8.72	36.20 – 34.66
Antarctic Intermediate Water	AAIW	567 – 1060	8.72 – 3.46	34.66 – 34.42
Circumpolar Deep Water	CDW	1060 – 1300	3.46 – 3.31	34.42 – 34.59
North Atlantic Deep Water	NADW	1300 – 3260	3.31 – 2.04	34.59 – 34.87
Antarctic Bottom Water	AABW	3260 to the bottom	< 2.04	–

Source: Adapted from STRAMMA; ENGLAND, 1999.

The South Atlantic has a very specific role in the ocean circulation, since it promotes the passage of water masses between the oceans in a general way. In this context, the bottom circulation pattern in the Brazilian continental margin is promoted by a series of deep currents located in the western portion of the ocean, which are composed of water masses from polar regions (REID, 1989). According to Broecker (2003), surface waters from other oceans (i.e. Indian and Pacific oceans) enter the South Atlantic and are eventually transported to the North Atlantic. When passing through the equatorial portion of the Atlantic, these waters are heated and, due to evaporation, become more saline. When they reach higher latitudes in the northern hemisphere, these warmer waters release heat into the atmosphere and, because they have a higher concentration of salt compared to local waters, they become heavier and sink. The water mass that is formed from this sinking, the NADW, flows to the South Atlantic, where it is redistributed through the regions of all ocean basins (BROECKER, 2003; HIRSCHI et al., 2003; THOMPSON; DANABASOGLU; PATTERSON, 2015), configuring, thus, the deep circulation of the Atlantic Meridional Overturning Circulation (AMOC), the Atlantic component of the thermohaline circulation (Figure 8).

Figure 8 – Illustrative diagram of the thermohaline circulation of the oceans (Atlantic, Indian and Pacific). The numbers on arrows correspond to water mass fluxes in Sverdrups (Sv)

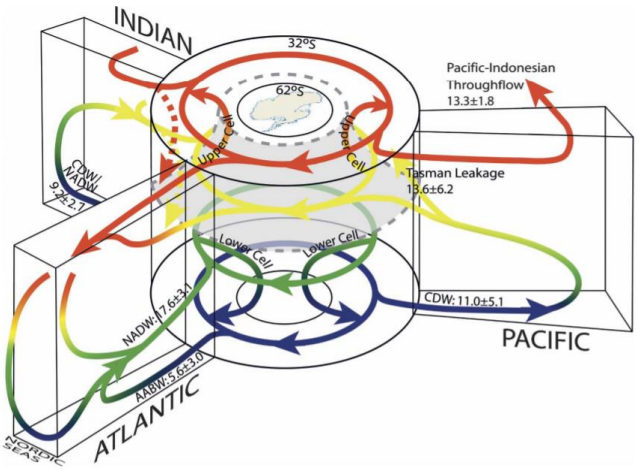

Source: LUMPKIN; SPEER, 2007.

The NADW is transported to the South Atlantic through the Deep Western Boundary Current (DWBC) over the western Atlantic margin at mid- to deep depths. However, after approximately 8°S, the continuous flow of DWBC is interrupted and the NADW transport is completed by vortex migration (DENGLER et al., 2004) (Figure 9).

Figure 9 – Schematic representation of surface (red arrows) and deep circulation (blue arrows) on the WEA. The currents indicated in the figure are South-Equatorial Current (SEC), Northern Brazil Current (NBC), Equatorial Undercurrent (EUC), North-Equatorial Undercurrent (NEUC), North-Equatorial Countercurrent (NECC) Deep Western Boundary Current (DWBC)

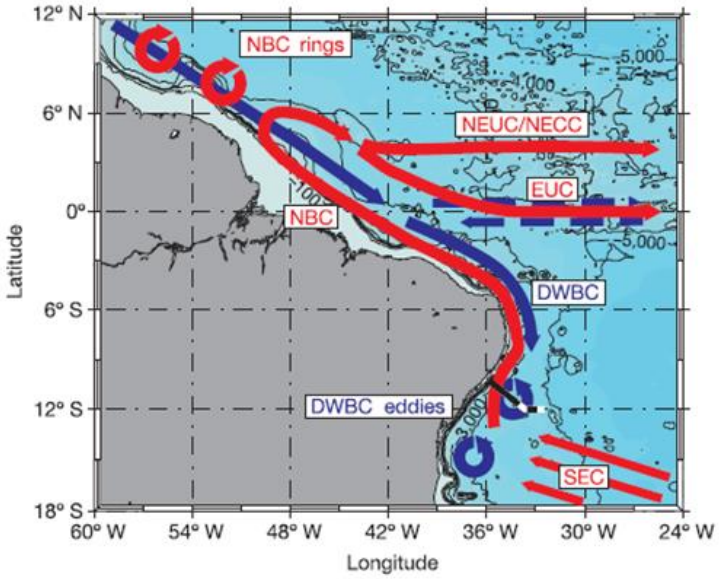

Source: DENGLER et al., 2004.

4 REGIONAL SETTING

The location of core GL-1248 (0°55.2'S, 43°24.1'W, 2,264 m depth) is in the WEA region, which is influenced by input of modern terrigenous sediments from northeastern Brazil (NACE et al., 2014; ZHANG et al., 2015) via the Parnaíba River, one of the most important drainage basins of northeast Brazil, occupying an area of 333,056 km^2 (3.9% of Brazilian territory). This river is about 1400 km long, and it is formed by the confluence of the minor rivers Água Quente and Lontra do Piauí, on the border of the states of Piauí, Maranhão, Tocantins and Bahia (AQUINO DA SILVA et al., 2015). At its mouth, it is formed the Delta do Parnaíba, in an environment dominated by waves and with important influences of the tides (SZCZYGIELSKI et al., 2014).

Zhang et al. (2015) observed, over the last 30 kyr, no Amazon-sourced terrigenous contribution for a nearby site due to the efficiency of the North Brazil Current (NBC) northwestward transport. From this observation, it is assumed that GL-1248 site is entirely controlled by input from the Parnaíba River, without influence of the Amazon River, even when the NBC is considerably weaker. The rainy season over the Parnaíba catchment is mainly driven by southward shifts of the Intertropical Convergence Zone (ITCZ), which reaches its southernmost extension over the northern portion of the basin during the months of March and April, when the intensity of northeast (NE) trade wind increases considerably (HASTENRATH, 2011).

The surface ocean circulation in the WEA region is predominantly influenced by the NBC, which is the northern branch of the South Equatorial Current (SEC) after its bifurcation around 10ºS (SCHOTT; STRAMMA; FISCHER, 1995; STRAMMA; FISCHER; REPPIN, 1995). The path of the NBC is the main passage in the WEA for the northwestern transport of upper-ocean warm saline waters across the equator (GONI; JOHNS, 2001). The velocity and volume of the water transported by the NBC depend on seasonal variations in the trade wind system (HASTENRATH; MERLE, 1987), with a minimum measured transport of approximately 13 Sv (1 Sv = 10^6 $m^3.s^{-1}$) occurring during the austral fall and a maximum transport about 36 Sv during the austral winter (JOHNS et al., 1998).

The WEA is also the main pathway for the Atlantic mid- and deep waters, wrapping them up into narrow basins surrounded by the Mid-Ocean Ridge and the South American Continental

Margin (GRÖGER; HENRICH; BICKERT, 2003). Today, the mid-depths of the continental slope off northeastern Brazil are bathed by southward flowing NADW (LUX; MERCIER; ARHAN, 2001; SCHOTT et al., 2003) that is transported along the Deep Western Boundary Current (DWBC), one of the most important components of the global oceanic thermohaline circulation (RHEIN; STRAMMA; SEND, 1995). The NADW transport via the DWBC occurs at a depth of between 1,200 and 2,500 m, reaching approximately 11 Sv (SCHOTT et al., 2003), whereas, in terms of velocity, the shallow upper NADW (around 1600 m) exceeds only 15 $cm.s^{-1}$ near 1°50'S (RHEIN; STRAMMA; SEND, 1995). In terms of the $[O_2]$, the present-day oxygen concentration at the depth of GL-1248 site is estimated to be approximately 250 $\mu mol.kg^{-1}$ (KEY et al., 2004). Thus, this sampling site is ideal to monitor the evolution of key-water mass properties of the lower limp of the AMOC.

5 MATERIAL AND METHODS

5.1 SAMPLING AND AGE MODEL

Sediment core GL-1248 (1,929 cm length) (Figure 10) was collected by Petrobras oil company in the offshore portion of the Barreirinhas Basin. The core was recovered near to the mouth of the Parnaíba River on the northern Brazilian continental slope about 160 km away from the modern coastline and at a water depth of 2,264 m (Figure 11). The core GL-1248 is characterized by greenish sediments, which are rich in silty clay and contains some carbonate-rich layers, represented by more reddish-brown and whitish clays.

Figure 10 – Lithofaciologic description of the sediments recovered from the core GL-1248 in the Barreirinha Basin.

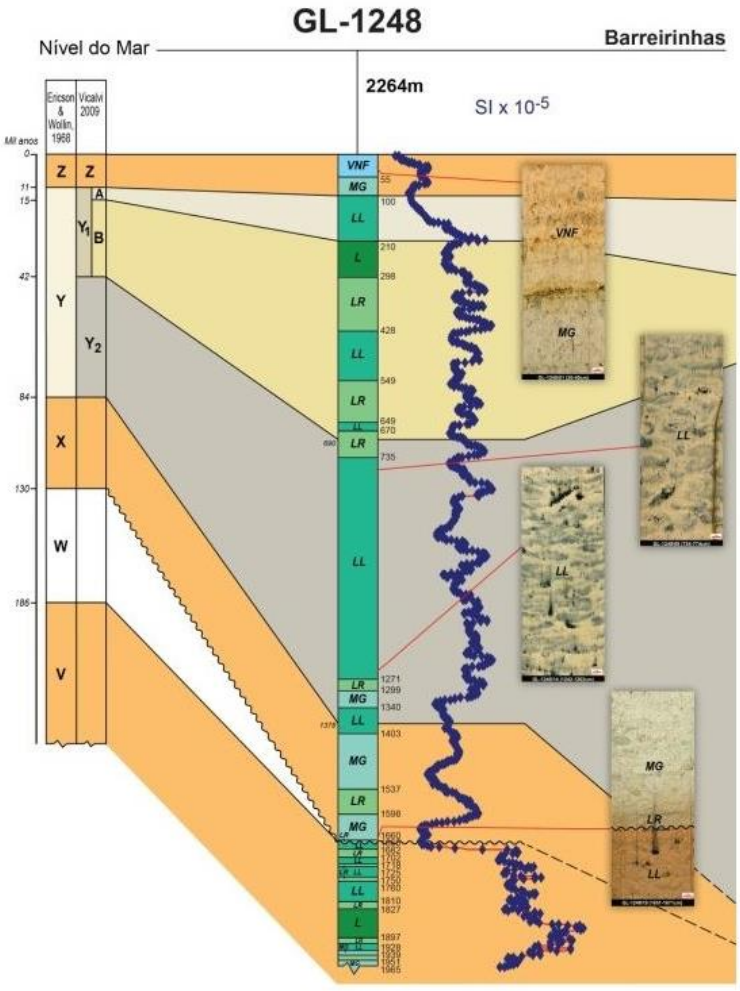

Source: Adapted from Ericson & Wollin (1968).

Figure 11 – (a) Map and (b) sea water [O_2] profile (in µmol.kg^{-1}) from the modern Atlantic Ocean showing the location of the core used in this work, GL-1248 (0°55.2'S, 43°24.1'W, 2,264 m), along with other core sites discussed in the text: SU90-03 (CHAPMAN; SHACKLETON, 1998), GeoB3910 (BURCKEL et al., 2015), KNR191-CDH19 (HENRY et al., 2016) and MD95-2042 (HOOGAKKER et al., 2015). AAIW stands for Antarctic Intermediate Water, NADW stands for North Atlantic Deep Water and AABW stands for Antarctic Bottom Water. Both figures were created using the software Ocean Data View software (SCHLITZER, 2017).

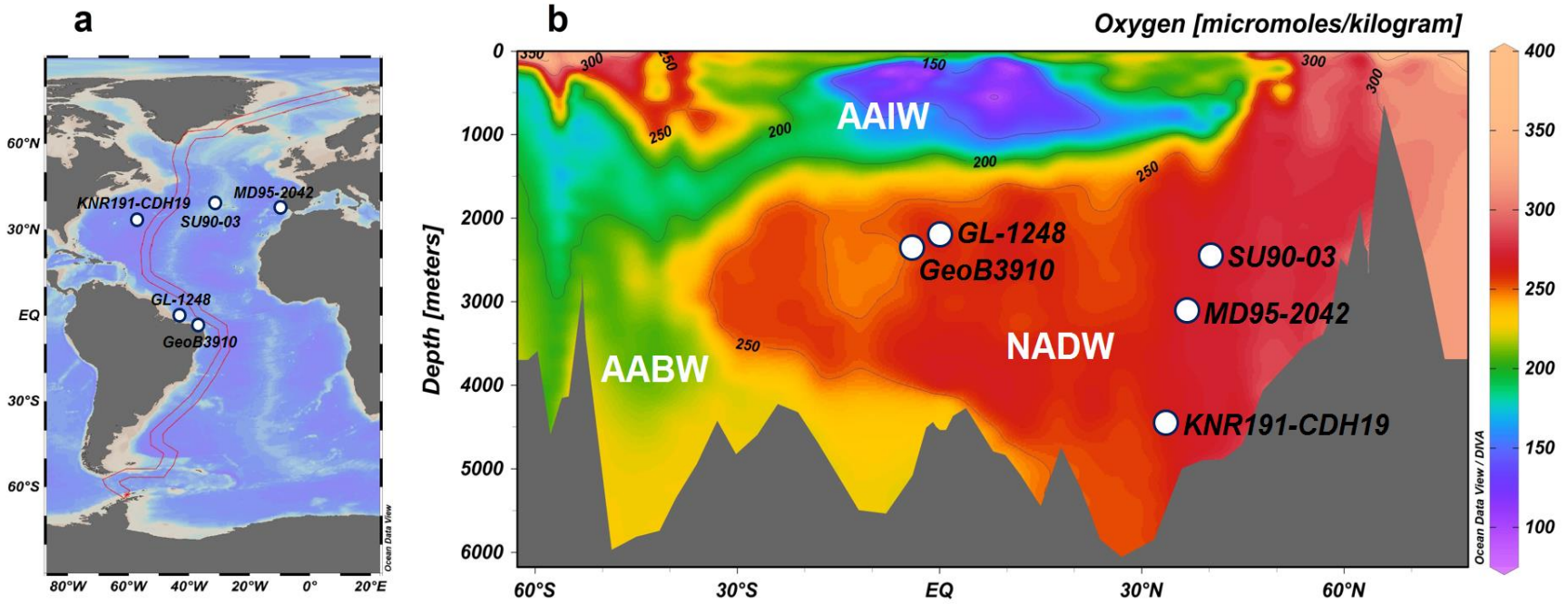

Source: GONÇALVES, 2019.

GL-1248 reaches approximately 128.7 kyr, according to the age-depth model previously developed by Venancio et al. (2018), with the mean sedimentation rate equals to 21 cm/kyr. This age-depth model is based on 12 AMS radiocarbon analyses performed on samples containing *Globigerinoides ruber* (white) and *Trilobatus sacculifer* in the upper 6.30 m of the core depth. The radiocarbon ages were calibrated with the IntCal13 calibration curve (REIMER et al., 2013). For the lower part of core GL-1248 (below 6.30 m core depth), the chronology was derived from the alignment of the Ti/Ca data from the core to the ice $\delta^{18}O$ record of the North Greenland Ice Core Project (WOLFF et al., 2010). The downcore ages were modeled using the package Clam 2.2 (BLAAUW, 2010).

Although the GL-1248 core covers the last glacial-interglacial cycle, only the last glacial period (between ~ 63 and 29 kyr) was analyzed in this work because this period encompasses several Heinrich Stadial (HS) events and, therefore, changes in the strength of the AMOC, required for the objectives of this study.

5.2 STABLE CARBON ISOTOPES ($\delta^{13}C$) ANALYZES IN BENTHIC FORAMINIFERA

Stable carbon isotopes ($\delta^{13}C$) were analyzed in 1 to 10 tests of epifaunal *Cibicides wuellerstorfi* and shallow infaunal *Uvigerina peregrina* from a >150 μm-sieved size fraction. Regarding the deep infaunal species *Globobulimina affinis*, the stable isotopic $\delta^{13}C$ signature was analyzed in 1 to 8 tests of those specimens (also > 150 μm). The analyses were performed with a Finning MAT 252 mass spectrometer with reproducibility lower than ±0.07‰ for $\delta^{13}C$ measurements over the period of the analyses. The isotopic data were adjusted relative to the Vienna Pee Dee Belemnite (VPDB) using the NBS 19 and UCD-SM92 calcite standards.

To reconstruct the bottom-water [O_2] content, it was used the gradient ($\Delta\delta^{13}C$) determined from the $\delta^{13}C$ measurements of the deep infaunal *G. affinis*, which captures the pore water signal, and the epifaunal *C. wuellerstorfi*, which represents the bottom-water signal, both from the same sediment samples. The gradient was converted into bottom-water [O_2] via a linear relationship between the carbon isotope gradient and the bottom-water [O_2], using the equation of Hoogakker et al. (2015) that is based on modern benthic carbon isotope ratios from core tops of the major ocean basins (Figure 12). The associated error in the [O_2] reconstruction method is ±17 $\mu mol.kg^{-1}$ (HOOGAKKER et al., 2015), and uncertainties related to the $\delta^{13}C$ measurements contribute an

error of ±10 μmol.kg^{-1} in the bottom-water [O_2] reconstruction. Hereafter, this carbon isotope gradient is referred to $\Delta\delta^{13}C_{C.wu\text{-}G.af}$.

Figure 12 – Relationship between $\Delta\delta^{13}C$ and [O_2] for the three major oceans

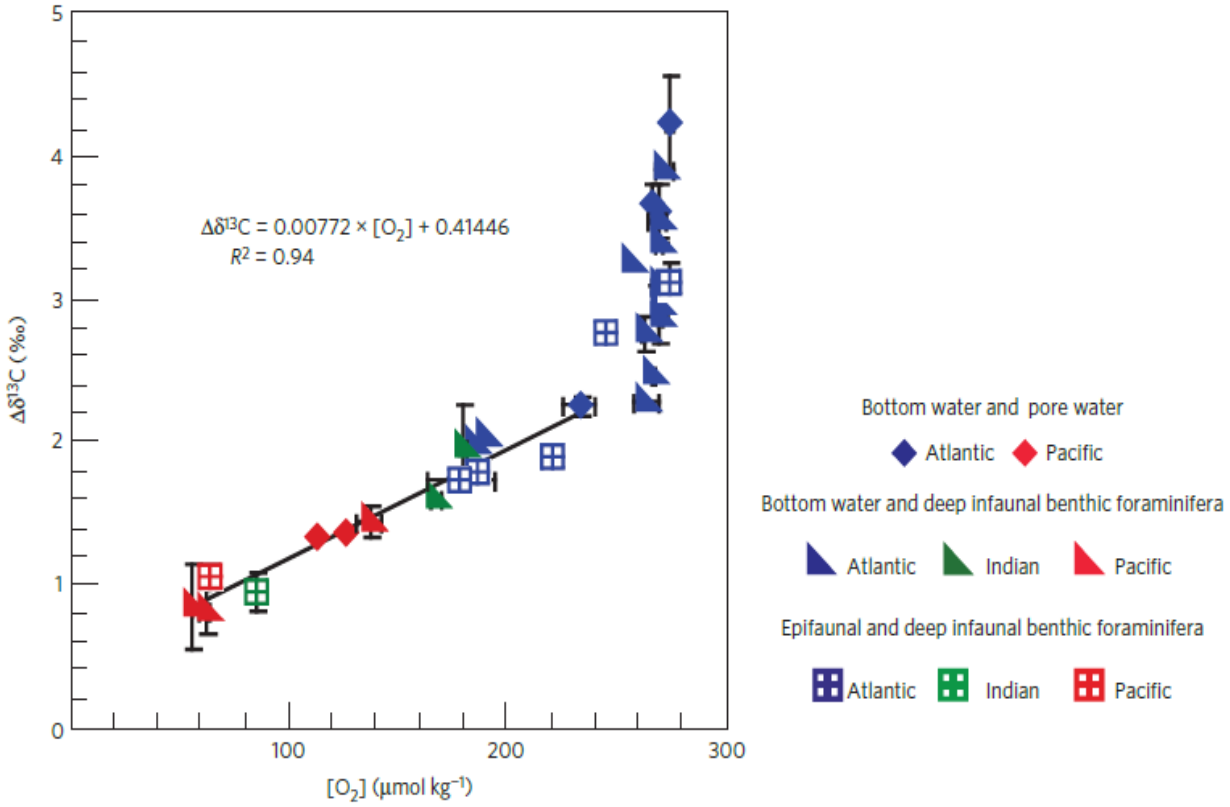

Source: HOOGAKKER et al., 2015.

It was also calculated the gradient between the $\delta^{13}C$ of the shallow infaunal *U. peregrina* and the epifaunal *C. wuellerstorfi* species from the same sediment sample as a proxy for regional contrasts in organic matter fluxes and the $\delta^{13}C$ associated with the pore water (MACKENSEN et al., 2017; THEODOR et al., 2016), denoted as $\Delta\delta^{13}C_{U.pe.\text{-}C.wu}$.

5.3 SEDIMENTOLOGICAL AND PALEOPRODUCTIVITY ANALYZES

Grain-size measurements in GL-1248 were determined in a particle analyzer via laser diffraction (CILAS 1064), which has a detection range of 0.02–2000 μm. The analysis was performed at a 5-cm resolution using decarbonated and organic matter-free samples via addition of HCl 1M and 30% hydrogen peroxide, respectively. Additionally, sodium hexametaphosphate

solution (4%) was added for particle dispersion. The results were calculated using the software routine GRADISTAT 1.0 (BLOTT; PYE, 2001) following the Wentworth scale for size classification. From these data, the mean size of the 'sortable silt' fraction (denoted by $\overline{SS}$, mean of 10–63 μm) was determined as a proxy for the intensity of the bottom-water currents (BIANCHI et al., 1999; MCCAVE; MANIGHETTI; ROBINSON, 1995). The percentages of the total organic carbon (TOC) were also determined in carbonate-free samples and analyzed using an Elementar Vario EL Cube elemental analyzer interfaced to a PDZ Europa 20-20 isotope ratio mass spectrometer.

Ti, Ca and other elements intensities were measured by Venancio et al. (2018) by employing nondestructive, profiling X-Ray Fluorescence (XRF) spectrometry. The measurements of the intensities were made by scanning the split surface of the core archive with an AVAATECH XRF core-scanner at intervals of 0.5 cm, by irradiating a surface of about 120 mm^2 at 10 kV for 20s. By using this automated scanning method, it was possible to determine the Ti/Ca ratio at very high resolution as a way to investigate fluvial terrigenous input for that area.

As an indicator of surface productivity, it was determined the relative abundance of three planktonic foraminifera that inhabit regions with high phytoplanktonic density (*Neogloboquadrina dutertrei*, *Neogloboquadrina incompta* and *Globigerina bulloides*). For this approach, dry > 63-μm sediment was sieved through a 150 mesh and split until at least 300–500 of the planktonic foraminifera specimens remained. The relative abundance of the productivity-related species was summed and measured at a downcore resolution of 10 cm. Species were identified and counted according to the methods of Loeblich & Tappan (1988) and Schiebel & Hemleben (2017).

5.4 INTEGRATION AND COMPARISON OF DATA

In order to corroborate the idea of this work, the data from core GL-1248 was compared to other studies from different locations of the Atlantic Ocean (Table 2). For the core SU90-03 and GeoB3910, it was used the benthic foraminifera $\delta^{13}C$ for comparison, while for the core KNR191-CDH19 it was used the $^{231}Pa/^{230}Th$ record. Additionally, it was used the $\Delta\delta^{13}C_{C.wu\text{-}G.af}$ from the core MD95-2042 for further comparison.

Table 2 – Identification and location of the cores collected in the Atlantic Ocean used for comparison with this study

Core	Latitude	Longitude	Depth	Studies
SU90-03	40º 03’ N	32º 00’ W	2,475 m	CHAPMAN; SHACKLETON, 1998
GeoB3910	04º 15’ S	36º 21’ W	2,362 m	BURCKEL et al., 2015
KNR191-CDH19	33º 41’ N	57º 35’ W	4,541 m	HENRY et al., 2016
MD95-2042	37º 48’ N	10º 10’ W	3,146 m	HOOGAKKER et al., 2015
GL-1248	00º 55’ S	43º 24’ W	2,264 m	this study

Source: Elaborated by the author, 2019.

6 RESULTS

6.1 AGE MODEL

Radiocarbon dating for core GL-1248 suggest an age of about 44.0 ± 0.7 kyr at 6.30-m core depth, and 128.7 kyr at 16.66-m core depth for the bottom age. The mean sedimentation rate is 21 cm/kyr, with higher values reaching 67 cm/kyr and lower values under 10 cm/kyr. However, the very low sedimentation rate (~ 3 cm/kyr) between 2.18- and 1.70-m core depth (29.1 and 14.8 kyr, respectively) is unusual for this region and period, suggesting the presence of a hiatus, even though no significant change in lithology is observed (Figure 13).

Figure 13 – GL-1248 age-depth model and sedimentation rates

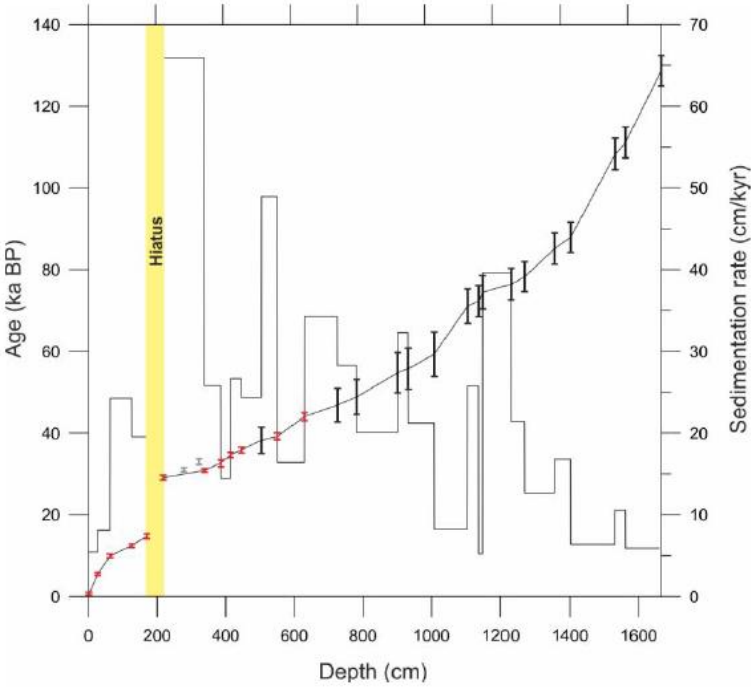

Source: VENANCIO et al., 2018.

6.2 STABLE CARBON ISOTOPES ($\delta^{13}C$), GRADIENTS ($\Delta\delta^{13}C$) AND BOTTOM-WATER RECONSTRUCTION

The carbon isotopes ($\delta^{13}C$) of *Cibicides wuellerstorfi* ranged from -0.21 to 1.60 ‰, with depleted $\delta^{13}C$ values occurring during HS (Figures 14c and 15c), especially during HS3 (-0.21

‰) and HS4 (0.20 ‰), indicating a marked reduction in water mass ventilation. For *Uvigerina peregrina*, the $\delta^{13}C$ values ranged from -1.76 to -0.02 ‰ (Figure 15c), also exhibiting the lowest values during HS, with its minimum during HS5a (-1.76 ‰). In the case of *Globobulimina affinis*, the $\delta^{13}C$ values ranged from -3.55 to -1.73 ‰ (Figure 15c) and, unlike the values for *C. wuellerstorfi*, some of the highest values occurred during HS, particularly during HS3 (-1.77 ‰) and HS5 (-1.87 ‰).

Figure 14 – Deep-water ventilation and bottom-current strength in the western equatorial Atlantic during HS over the last glaciation from the mid-depths. (**a**) *C. wuellerstorfi* $\delta^{13}C$ data from core SU90-03 (CHAPMAN; SHACKLETON, 1998) (green line and squares). (**b**) *C. wuellerstorfi* $\delta^{13}C$ data from core GeoB3910 (BURCKEL et al., 2015) (light blue line and squares). (**c**) *C. wuellerstorfi* $\delta^{13}C$ data from core GL-1248 (this study) (dark blue line and circles). (**d**) $^{231}Pa/^{230}Th$ records from core KNR191-CDH19 (HENRY et al., 2016) (pink line and triangles). The pink dotted line represents the $^{231}Pa/^{230}Th$ production rate of 0.093. (**e**) Sortable silt ($\overline{SS}$) records from core GL-1248 (this study) (orange line and circles). Grey bars represent millennial cold events (HS3, HS4, HS5, HS5a and HS6)

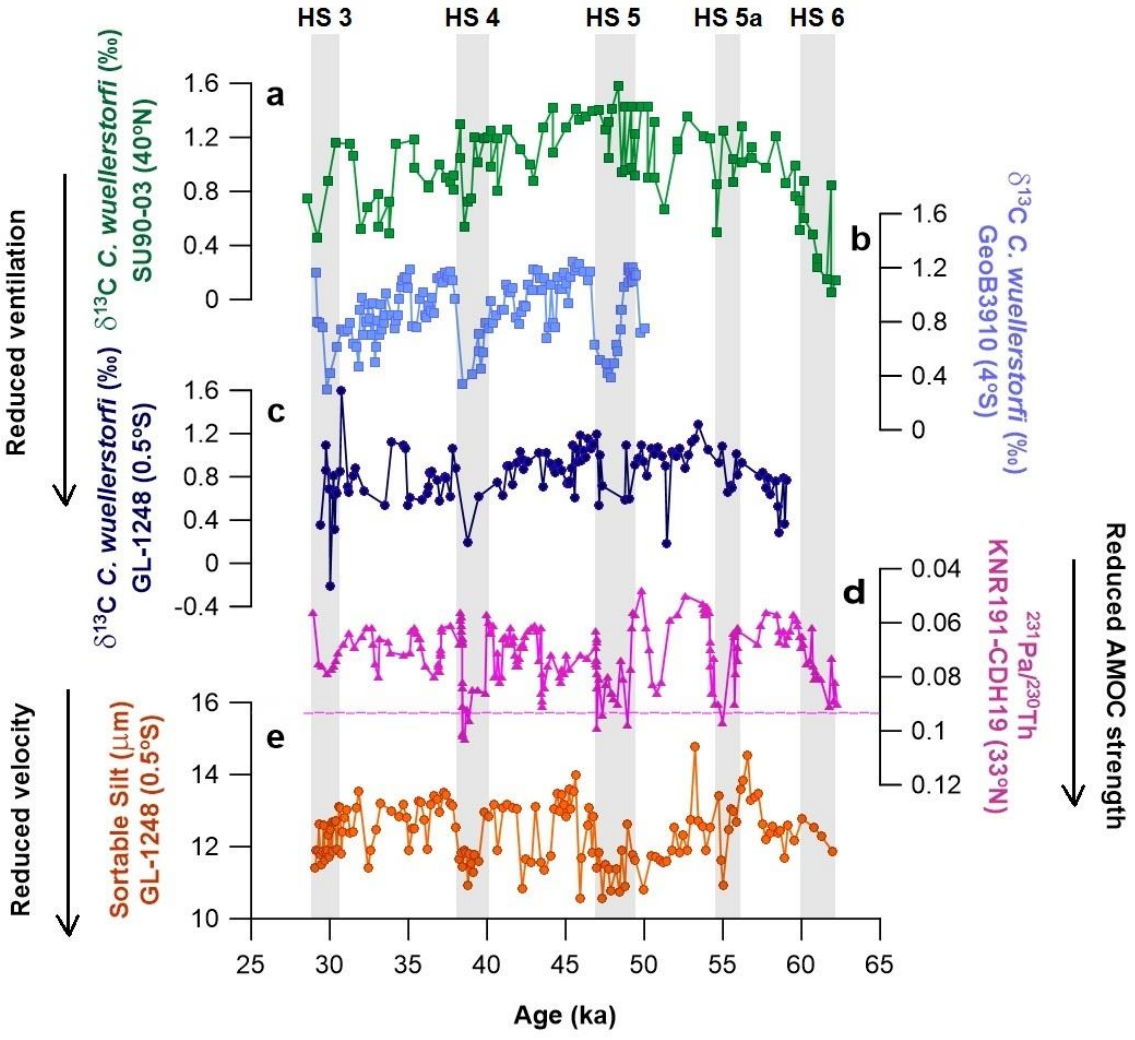

Source: GONÇALVES, 2019.

The values for the bottom-water [O_2], calculated by applying the $\Delta\delta^{13}C_{C.wu\text{-}G.af}$: [O_2] calibration equation, ranged from 449 to 241 μmol.kg^{-1} (Figure 15f), showing lower values during HS3 and HS4 (241 and 247 μmol.kg^{-1}, respectively). From these values, it was possible to conclude that the bottom-water [O_2] for the period covered was not completely poorly-oxygenated, as the threshold concentration for well-oxygenated waters should be at least > 235 μmol.kg^{-1} (HOOGAKKER et al., 2015; MCCORKLE; EMERSON, 1988). However, if considered the associated error (±17 μmol.kg-^{1}), these values can indicate poorly-oxygenated waters. On the other hand, to be considered hypoxic, [O_2] values must reach 60 μmol.kg^{-1}, although this value can vary depending on some parameters, such as temperature and CO_2 availability (HOOGAKKER; THORNALLEY; BARKER, 2016; KEELING; KÖRTZINGER; GRUBER, 2010). Regarding the $\Delta\delta^{13}C_{U.pe\text{-}C.wu}$ values for GL-1248 site, the proxy does not show a specific pattern among the HS as indicated by other parameters (Figure 15e) mostly because both *C. wuellerstorfi* and *U. peregrina* show negative $\delta^{13}C$ anomalies during HS, with values ranging from 0.37 to 2.13 ‰.

6.3 SEDIMENTOLOGICAL AND PALEOPRODUCTIVITY ANALYZES

The grain size analyses revealed $\overline{SS}$ mean values ranging from 10.56 to 14.76 μm (Figure 14e). The lowest values were observed during all of the HS, which provides evidence for weakened bottom current strength at the core location. The TOC content of the core varied between 0.56 and 1.15 % (Figure 15b). TOC accumulation rates were highest during HS4, but also showed a remarkable increase during HS5, probably due to a higher input of organic matter from the continent (ARZ; PÄTZOLD; WEFER, 1998).

The Ti/Ca ratio ranged between 0.0079 and 0.6796 (Figure 15a). The highest ratios were observed during the HS, especially in the beginning of HS3 and middle of HS5. Exception occurred for the HS6, which did not present high values as expected.

The relative abundance of the productivity-linked planktonic foraminifera ranged from 5.69 to 31.85 % (Figure 15d) with low values occurring, in general, during HS (more pronounced during HS3 and HS5a) and between 56 and 47 kyr. The highest values mostly occurred after the end of the stadials, with the exception of HS5a, which was preceded by a phase of high abundance.

Figure 15 – Bottom-water [O_2] reconstruction in the western equatorial Atlantic during HS over the last glacial period at the mid-depths. (**a**) Ti/Ca ratios from core GL-1248 (VENANCIO et al., 2018) (brick red line), used as an indicator for HS. (**b**) Total organic carbon (TOC) from core GL-1248 (this study) (brown line and squares). (**c**) Benthic foraminifera $\delta^{13}C$ from core GL-1248 (this study) (dark blue, pink and light green lines and circles). (**d**) Planktonic foraminifera productivity species from core GL-1248 (this study) (yellow line and diamonds). (**e**) $\Delta\delta^{13}C_{U.pe\text{-}C.wu}$ from core GL-1248 (this study) (red line and circles). (**f**) $\Delta\delta^{13}C_{C.wu\text{-}G.af}$ and reconstruction of bottom-water oxygen content ([O_2]) from core GL-1248 (this study) (black line and circles). The black dotted line represents the threshold of 235 µmol.kg^{-1} for suboxic [O_2] conditions. (**g**) $\Delta\delta^{13}C_{C.wu\text{-}G.af}$ from core MD95-2042 (HOOGAKKER et al., 2015) (purple line and triangles). Grey bars represent millennial cold events (HS3, HS4, HS5, HS5a and HS6)

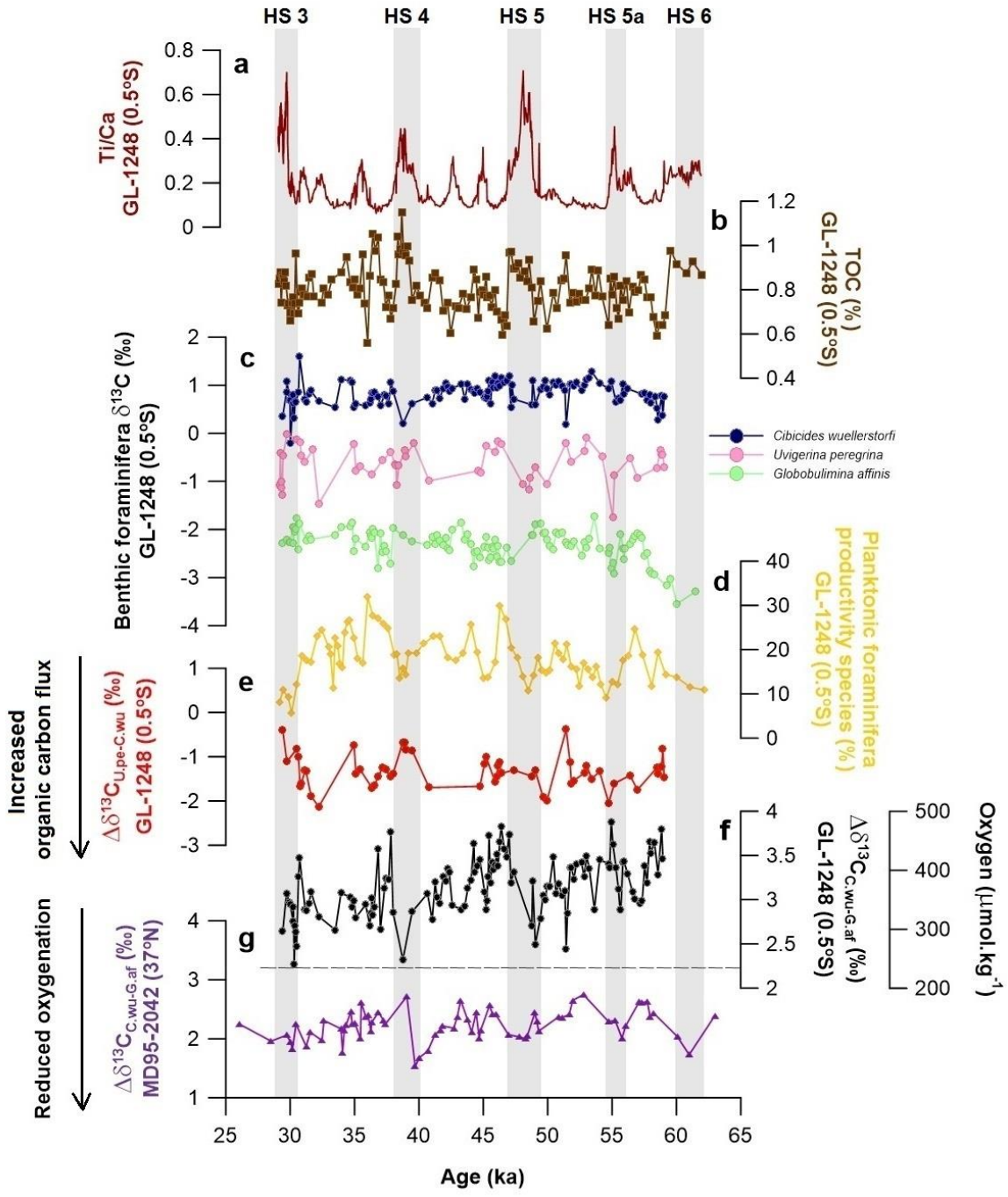

Source: GONÇALVES, 2019.

7 DISCUSSION

7.1 DEEP-WATER VENTILATION AND BOTTOM-CURRENT STRENGTH IN THE WEA

The $\delta^{13}C$ of epifaunal benthic foraminifera, in general, indicates a 1:1 proportion in the variability of the $\delta^{13}C$ of the dissolved inorganic carbon ($\delta^{13}C_{DIC}$) (WOODRUFF; SAVIN; DOUGLAS, 1980; ZAHN; WINN; SARNTHEIN, 1986). However, variations in the $\delta^{13}C$ of these species may not be entirely related to variations in this proportion (GOTTSCHALK et al., 2016b), but also could be caused by environmental effects, such as microhabitat variations of the species (CORLISS, 1985; TACHIKAWA; ELDERFIELD, 2002), changes in the carbonate system (SPERO et al., 1997), CO_2 exchange between the ocean and atmosphere (PIOTROWSKI et al., 2008), and exported productivity. Changes in primary production, for example, can lead to higher remineralization rates in the sediment, which is reflected in the $\delta^{13}C$ signal of the epifaunal foraminifera species (CURRY; LOHMANN, 1983; LACERRA et al., 2017). Hence, the lower $\delta^{13}C$ values in epifaunal foraminifera species could reflect seasonal variations in the primary productivity from the surface waters to the bottom-waters (MACKENSEN et al., 1993). However, when it comes to the *Cibicides wuellerstorfi* species, this situation can be different in some ways. These specimens have an epibenthic habitat by living above or within the upper region of the phytodetritus layer, where the effect of the remineralization of the exported carbon is non-existent or minimal (CORLISS et al., 2006; GOTTSCHALK et al., 2016b). In general, this species prefers a low organic carbon flux to live (MACKENSEN et al., 1995), and its carapace is formed in moments of enrichment of ^{13}C in bottom-waters (GOTTSCHALK et al., 2016b). The data based on the *C. wuellerstorfi* $\delta^{13}C$ show negative carbon excursions during HS in the WEA, most clearly identified in HS3 and HS4 (Figures 14c and 15c); however, the depletion of the *C. wuellerstorfi* $\delta^{13}C$ signal at GL-1248 site may have no influence with the carbon flux, either that produced on the surface or that from continent. This assumption is consistent with the study of Voigt et al. (2017), who showed a tight decoupling between the detritus input from the continent and the mid-depth $\delta^{13}C$ anomaly in the WEA during HS1. From these observations, it is proposed that the same pattern occurred during the other HS. Nevertheless, the *C. wuellerstorfi* $\delta^{13}C$ values are broadly consistent with the tendency observed in the North Atlantic core SU90-03 (Figure 14a), where lower values during HS were associated with reorganizations of NADW production

(CHAPMAN; SHACKLETON, 1998). The results were also consistent with those from the nearby GeoB3910 core from Burckel et al. (2015), where changes in the bottom-water nutrient content and ventilation during HS were reported (Figure 14b), as well as the MD09-3275 core from Waelbroeck et al. (2018), in which changes in ocean ventilation during HS were also observed, particularly during HS1, HS4 and HS5.

In addition to the increase in terrigenous organic carbon and the exported productivity, the $\delta^{13}C$ records found in the intermediate-to-deep Atlantic can also be influenced by other parameters, such as changes in water masses mixing and sources or addition of respired organic carbon during these cold events. Oppo et al. (2018) observed that partial replacement of northern sourced deep-water by high-nutrient Antarctic Intermediate Water (AAIW) near the Demerara Rise in the western tropical North Atlantic could be a cause for changes in local subsurface water properties, e.g., phosphate concentration and carbonate saturation. However, using neodymium isotope measurements from cores throughout the Atlantic, Howe et al. (2016) showed that the low $\delta^{13}C$ values cannot be interpreted exclusively as changes in the sources of the water masses, and are rather the result of a large amount of respired carbon stored in deeper parts of the Atlantic during the Last Glacial Maximum (LGM). Furthermore, Voigt et al. (2017) stated that the negative $\delta^{13}C$ excursions in the Atlantic Ocean observed during H1 and the Younger Dryas are a reflection of an increase in the residence time of the northern water components, rather than an alternation or mixing of southern and northern water masses. This mechanism would then allow an accumulation of respired carbon in the mid-depths (~ 1000–3000 m), changing the $\delta^{13}C$ values to more negative ones due to increased oxygen consumption (KROOPNICK, 1985). From this, the depleted $\delta^{13}C$ values in *C. wuellerstorfi* are caused by reduced ventilation and not only due to circulation changes. Those changes are attributed to shifts in the intensity of the AMOC, which is a fundamental component responsible for determining the paths of deep and surface currents.

The $\overline{SS}$ data, a physical proxy for deep currents based on the main size of the silt fraction (BIANCHI et al., 1999; MCCAVE; MANIGHETTI; ROBINSON, 1995), exhibit an interesting pattern in the deep current velocity (Figure 14e). The data indicate that the lower values that occurred during HS, especially HS4 and HS5, can be interpreted as a decrease in the bottom-current strength. The variability is coeval to the $\delta^{13}C$ excursions of *C. wuellerstorfi*. On the other hand, higher $\overline{SS}$ values are related to a recovery of DWBC transport, which carries smaller particles from the $\overline{SS}$ fraction. The $\overline{SS}$ data are also broadly consistent with the $^{231}Pa/^{230}Th$ record

(a specific proxy for the strength of the AMOC) from the KNR191-CDH19 core (HENRY et al., 2016), which was recovered from the Bermuda Rise in the northwestern Atlantic Ocean (Figure 14d). During HS, the $^{231}Pa/^{230}Th$ ratio increases as consequence of decreased lateral export of ^{231}Pa, which is consistent with a reduced or shallower overturning cell in the North Atlantic (BÖHM et al., 2014; BURCKEL et al., 2016; MCMANUS et al., 2004). In conclusion, both $\delta^{13}C$ and $\overline{SS}$ at the GL-1248 site support the notion of low bottom-current advection and reduced NADW ventilation at the mid-depths during HS concomitant with a shallower or weakened AMOC in the WEA.

7.2 BOTTOM-WATER [O_2] RECONSTRUCTION IN THE WEA

Benthic foraminifera have different food and oxygen demands and, for this reason, live and calcify at different sediment depths. Infaunal species tend to have lower $\delta^{13}C$ values than epifaunal species growing at the same time and at the same location, mostly because the $\delta^{13}C$ of pore waters can be depleted in sediment with high rates of organic matter respiration (GROSSMAN, 1987; MACKENSEN et al., 2000; MCCORKLE; CORLISS; FARNHAM, 1997). In this sense, *C. wuellerstorfi* inhabits the sediment surface, while *G. affinis* lives in a low-oxygen microhabitat in sub-surface sediments that other species may not tolerate (CORLISS, 1985; CORLISS; EMERSON, 1990; GESLIN et al., 2004). The presence of this latter species (*G. affinis*) can indicate oxygen-limited conditions in which there is a high abundance of available organic carbon. The $\delta^{13}C$ gradient between both species can be used as a proxy for changes in the bottom-water oxygenation at different depths across the oceans, since the gradient reflects the difference between the signals of the bottom-water and pore water, respectively (MCCORKLE; EMERSON, 1988). In the Atlantic Ocean, however, the mechanisms involved are still not totally clear and may differ from one specific water depth to another.

In the deep- and mid-depths over the North Atlantic and Southern Ocean, the main cause for the glacial decreases in the bottom-water [O_2] are attributable to circulation changes and/or biological productivity (GOTTSCHALK et al., 2016a; HOOGAKKER et al., 2015; HOOGAKKER; THORNALLEY; BARKER, 2016). Hoogakker et al. (2015) attributed variations in the [O_2] during a series of HS and glacial cold events on the Iberian margin to ocean circulation changes, with a mixing between southern and northern water masses as a reflection of

AMOC slowdowns (Figure 15g). However, their site (MD95-2042) is located at a deeper depth of about 3,146 m. On the other hand, as discussed before, it was suggested that no significant shifts occurred between water masses at the mid-depths during the LGM in the WEA (HOWE et al., 2016; 2018; LAMBELET et al., 2016) and, therefore, such processes are likely not the main mechanism behind the changes in the bottom-water [O_2] during millennial-scale cold events in these regions.

Changes in primary production also lead to decreased bottom-water [O_2] values via the respiration processes. However, considering the distinct biological mechanisms involved, understanding these decreases can be challenging due to their complexity. Studies from different locations, including the equatorial region, have attributed increases in productivity at oligotrophic locations to opal booms during glacial periods and HS (BRADTMILLER et al., 2007; GIL; KEIGWIN; ABRANTES, 2009; MECKLER et al., 2013), which may have been caused by an enhanced silicate availability in the mixed subsurface layer due to weak stratification during HS (i.e. HS5) (HOOGAKKER et al., 2013). Portilho-Ramos et al. (2017) interpreted the change in primary productivity during HS1 to be a result of a shallow mixed layer depth that allowed the presence of cold and nutrient-rich thermocline waters very close to the surface. Vink et al. (2001) reported a pronounced change in calcareous dinoflagellate cyst accumulation and organic carbon deposition in response to changes in the NEC during the first five major HS over the last glacial period, which were associated with rapid changes in local productivity. Other studies, however, suggested different interpretations for these mechanisms. Hertzberg et al. (2016), for example, showed that the biological pump efficiency was reduced during HS1, leading to an initial CO_2 rise during the last deglaciation.

To assess the occurrence of enhanced productivity in the water column, it was analyzed the relative abundance of the planktic foraminifera species that strongly respond to this parameter (Figure 15d). In the GL-1248 core, the most important productivity-related species are *Neogloboquadrina dutertrei*, *Neogloboquadrina incompta* and *Globigerina bulloides*. Their abundance increases in response to the enhanced phytoplankton biomass resulting from blooms in waters with high nutrient concentrations (BOLTOVSKOY; BOLTOVSKOY; BRANDINI, 2000). At GL-1248 site, nutrients are inserted into a photic zone via shoaling (upwelling) of the thermocline (PORTILHO-RAMOS et al., 2017*).* *N. incompta* and *G. bulloides* are cold water and upwelling species, and they can be related to the uppermost shoaling of the thermocline in

the WEA (BOLTOVSKOY; BOLTOVSKOY; BRANDINI, 2000; UFKES; FRED JANSEN; BRUMMER, 1998). On the other hand, *N. dutertrei* prefers the uppermost thermocline layer in tropical waters near the equator, at the mouths of large rivers and at the outer borders of coastal upwelling areas (REBOTIM et al., 2017; UFKES; FRED JANSEN; BRUMMER, 1998). Based on these features, the results show that HS were periods of less intense primary productivity during the last glacial period, indicating only a minor influence on the decreased bottom-water [O_2] in the WEA.

The [O_2] reconstruction from the $\Delta\delta^{13}C_{C.wu\text{-}G.af}$ data suggests a decrease in the oxygen concentration during HS at mid-depths (Figure 15f), which is coincident with higher values of *G. affinis* $\delta^{13}C$ during HS3, HS4 and HS5 (Figure 15c) and the maximum accumulation of total organic carbon, especially during HS4 and HS5 (Figure 15b). However, during these periods of low oxygenation, the *G. affinis* $\delta^{13}C$ is not consistent with the increased abundance of respired carbon at GL-1248 site. Furthermore, the $\Delta\delta^{13}C_{U.pe\text{-}C.wu}$ values, a proxy used here as an indicator of carbon exportation, are also inconsistent with increased organic carbon flux during HS (Figure 15e). Moreover, the maximum accumulation of total organic carbon observed during HS was inversely related to the planktonic foraminifera productivity species, indicating that these peaks in total organic carbon did not arise from surface biological productivity, but possibly from continental river discharge. Thus, the changes in marine primary productivity are not the main cause of the [O_2] changes in the WEA.

The Ti/Ca data from core GL-1248 (VENANCIO et al., 2018) show a prominent input of terrigenous organic matter during HS (Figure 15a) as consequence of more humid climatic conditions over the northeast of the Brazilian continent (ARZ; PÄTZOLD; WEFER, 1998; JAESCHKE et al., 2007). Mulitza et al. (2017) observed increases in the iron to calcium ratios (Fe/Ca) during HS due to a migration of the ITCZ to southern regions in agreement to reductions in the AMOC. The input of terrigenous organic material from the continent during HS would have promoted an accumulation of respired carbon on the seafloor, preventing the diffusion of O_2 into the sediments and leading to a decrease in the *G. affinis* $\delta^{13}C$ at GL-1248 site due to increased light carbon availability. Through such a process, it was expect the same pattern for the $\Delta\delta^{13}C_{U.pe\text{-}C.wu}$, where an increased gradient would be observed during HS. However, this is not the case. The opposite is observed during periods between HS, where an increase in bottom-water ventilation at GL-1248 site favored remineralization and O_2 diffusion into the sediments,

propitiating the negative carbon excursion in the *G. affinis* $\delta^{13}C$ during HS. Here it is important to highlight that during HS3, HS4 and HS5, the $\Delta\delta^{13}C_{C.wu\text{-}G.af}$ data indicate well-defined, low [O_2] values, consistent with the lowest $\overline{SS}$ data. The decrease in the bottom-current flow and the low ventilation during these events could have favored the accumulation of organic carbon, especially during HS4 and HS5. For the total organic carbon and $\Delta\delta^{13}C_{C.wu\text{-}G.af}$ data, it was calculated a direct spatial correlation that showed an R^2 value of 0.41 (Figure 16), where an increase in organic carbon accumulation led to a decrease in the gradient between the *C. wuellerstorfi* and *G. affinis* $\delta^{13}C$ values. The increased TOC content, therefore, not only shows the entry/preservation of the carbon deposited on the slope during HS, but also a barrier of low O_2 diffusion in the sediment. For these reasons, it is proposed that the main mechanism behind the changes in bottom-water oxygenation at the mid-depths in the WEA is mainly caused by modifications in the ventilation during millennial-scale cold events, followed by deposition of continental organic carbon.

Figure 16 – Bivariate plot of the total organic carbon (TOC) (%) vs. the $\Delta\delta^{13}C_{C.wu\text{-}G.af}$ (‰) in core GL-1248 (this study) (R^2 = 0.41)

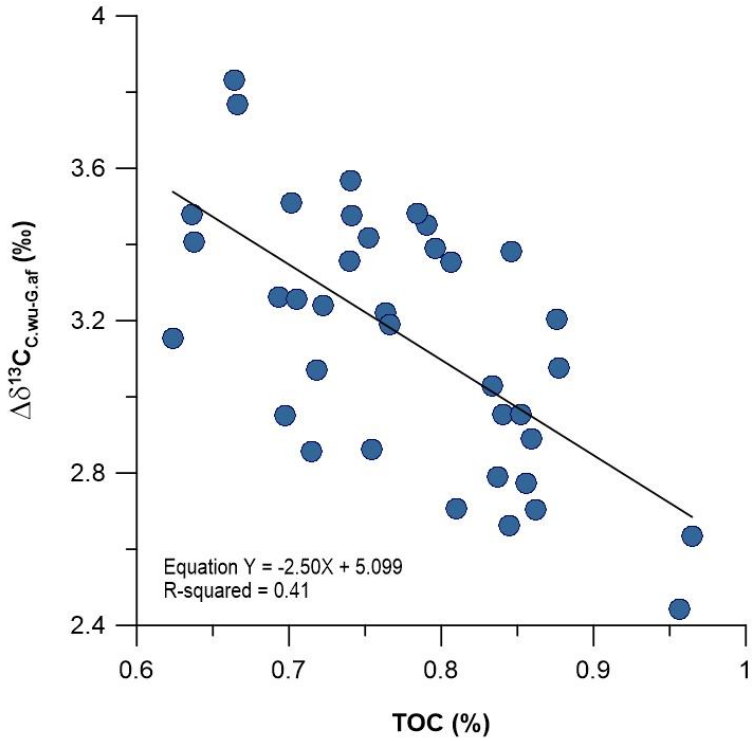

Source: GONÇALVES, 2019.

Interestingly, the $\Delta\delta^{13}C_{C.wu\text{-}G.af}$ record indicates a minor decrease in the oxygen content in the WEA during HS compared to those reported by Hoogakker; Thornalley & Barker (2016) at the NW Atlantic mid-depth ODP Site 1055 (1.8 km). These authors observed the lowest [O_2] values during the C21 and 19 millennial cool events (179 and 194 μmol.kg^{-1}, respectively) that occurred around 85 and 70 kyr (CHAPMAN; SHACKLETON, 1999), which they attribute to productivity changes from the surface ocean to the sediment and subsequent remineralization. It is important to emphasize that the [O_2] reconstruction, especially the peaks during HS3 (241 μmol.kg^{-1}), HS4 (247 μmol.kg^{-1}) and HS5 (270 μmol.kg^{-1}), do not show completely suboxic conditions. However, even though these values do not reach the sub-anoxia limit, when the associated error of ±17 μmol.kg-^{1} associated to the Hoogakker et al. (2015) equation is considered, the figures for HS3 and HS4 could indeed indicate suboxic conditions. Despite this possibility, the reconstruction is consistent with the model proposed by Schmittner et al. (2007). Via simulations of the oxygen cycle in response to changes in deep-water subduction across North Atlantic, they showed a decrease in the [O_2] below a depth of 1 km in the deep and mid-depths of the Atlantic that was related to extreme cold events. Nevertheless, Voigt et al. (2017) reinforced the idea that the modifications in oxygenated water masses were caused by biological respiration of organic matter, which is reflected in their Mn record (a specific tracer of redox conditions), since those waters were supplied with less oxygen during HS1 and HS2, indicating a less vigorous ventilation of northern sources across the WEA. Although their record is limited to the first two HS, it is possible that these redox conditions also occurred during another HS.

Finally, the results highlight the important role of the interactions between the atmosphere, continents and oceans for understanding the changes in the carbon cycle, such that the continent modifies the biogeochemical conditions on the ocean seafloor by supplying organic carbon and preventing O_2 diffusion into the sediments, processes that are crucial for the storage of atmospheric CO_2. In summary, it is believed that ocean ventilation coupled to organic carbon deposition at GL-1248 site were the main force behind the changes in the bottom-water [O_2] in the WEA, which had a fundamental role in carbon exportation and stock maintenance during millennial abrupt cold events.

8 CONCLUSIONS

From this study, it was possible to present a reconstruction of the mid-depth water [O_2] in the western equatorial Atlantic at a depth of 2,264 m based on the results of the $\Delta\delta^{13}C_{C.wu\text{-}G.af}$ from core GL-1248 and show that bottom-water oxygenation decreased during several HS (i.e. HS3, HS4 and HS5) across the last glacial period. The results support the idea that weaker circulation favored lower NADW ventilation in the WEA, leading to greater storage of respired carbon during these intervals. Consequently, low oxygen concentrations were observed during the HS due to significant increase in continental organic carbon input that reflects a decrease in the ocean circulation at GL-1248 site. It was suggested that the most important mechanism behind these oxygenation changes in the bottom-waters during HS was reduced ventilation coupled with increases in the abundance of organic carbon that prevented O_2 diffusion into the sediment instead of primary productivity from surface ocean. These findings reinforce the important role of biological and physical mechanisms driving Atlantic seawater [O_2] changes during cold stadial events over the last glacial period.

Considering the above conclusions, it can be inferred that the hypotheses proposed in this study can be accepted according to the geochemical, sedimentological, micropaleontological and isotopic results obtained, showing the influence of the NADW ventilation on the changes in the benthic foraminifera isotopic signal, as well as the relation between the periodic variation of the AMOC and the changes in the bottom-waters oxygenation during the last glacial period. However, the conceptual model initially proposed is not totally adequate, since the expected pattern for the $\Delta\delta^{13}C_{U.pe\text{-}C.wu}$, where an increased gradient would be observed during HS, did not happen as a result of possible different sources of organic carbon during these periods.

Finally, it is suggested that future studies involving a high-resolution multiproxy approach can be extended to the entire equatorial region of the Atlantic in order to improve the understanding of the relation between the physical mechanisms of the AMOC and the processes that govern changes in bottom-water oxygenation, besides helping to better understand the dynamics of this cell and its importance in the control of redox changes in low latitudes.

9 REFERENCES

ADKINS, J. The salinity, temperature, and $\delta^{18}O$ of the glacial deep ocean. **Science**, v. 298, n. 5599, p. 1769-1773, 2002.

ADKINS, J. The role of deep ocean circulation in setting glacial climates. **Paleoceanography**, v. 28, n. 3, p. 539-561, 2013.

AQUINO DA SILVA, A. et al. The influence of climatic variations on river delta hydrodynamics and morphodynamics in the Parnaíba Delta, Brazil. **Journal of Coastal Research**, v. 314, p. 930-940, 2015.

ARENILLAS, I. **Foraminíferos:** biologia, organización de la concha y classificación. 2nd ed. Zaragoza: Prensas Universitarias de Zaragoza, 2004. 126 p.

ARMSTRONG, H.; BRASIER, M. **Microfossils, stable isotopes and ocean-atmosphere**. 2nd ed. Oxford: Blackwell Publishing, 2005.

ARZ, H.; PÄTZOLD, J.; WEFER, G. Correlated millennial-scale changes in surface hydrography and terrigenous sediment yield inferred from Last-Glacial marine deposits off Northeastern Brazil. **Quaternary Research**, v. 50, n. 02, p. 157-166, 1998.

BANDY, O.; ARN, R. Distribution of recent foraminifera off west coast of Central America. **AAPG Bulletin**, v. 41, 1957.

BERGER, W.; WEFER, G. Export production: seasonality and intermittency, and paleoceanographic implications. **Palaeogeography, Palaeoclimatology, Palaeoecology**, v. 89, n. 3, p. 245-254, 1990.

BERNHARD, J. Characteristic assemblages and morphologies of benthic foraminifera from anoxic, organic-rich deposits: Jurassic through Holocene. **The Journal of Foraminiferal Research**, v. 16, n. 3, p. 207-215, 1986.

BIANCHI et al. Measurement of the sortable silt current speed proxy using the Sedigraph 5100 and Coulter Multisizer IIe: precision and accuracy. **Sedimentology**, v. 46, n. 6, p. 1001-1014, 1999.

BIGNOT, G. **Los microfossiles. Aplicaciones paleobiológicas y geológicas**. Madri: Paraninfo S.A., 1988.

BLAAUW, M. Methods and code for 'classical' age-modelling of radiocarbon sequences. **Quaternary Geochronology**, v. 5, n. 5, p. 512-518, 2010.

BLOTT, S.; PYE, K. GRADISTAT: a grain size distribution and statistics package for the analysis of unconsolidated sediments. **Earth Surface Processes and Landforms**, v. 26, n. 11, p. 1237-1248, 2001.

BÖHM, E. et al. Strong and deep Atlantic meridional overturning circulation during the last glacial cycle. **Nature**, v. 517, n. 7532, p. 73-76, 2014.

BOLTOVSKOY, E. **Los foraminíferos recientes:** Biologia, métodos de estúdio, aplicación oceanográfica. Buenos Aires: Editorial Universitaria de Buenos Aires, 1965.

BOLTOVSKOY, E.; BOLTOVSKOY, D.; BRANDINI, F. Planktonic foraminifera from southwestern Atlantic epipelagic waters: abundance, distribution and year-to-year variations. **Journal of the Marine Biological Association of the UK**, v. 80, n. 2, p. 203-213, 2000.

BOND, G. et al. Evidence for massive discharges of icebergs into the North Atlantic Ocean during the last glacial period. **Nature**, v. 360, n. 6401, p. 245-249, 1992.

BRADTMILLER, L. et al. Opal burial in the equatorial Atlantic Ocean over the last 30 ka: Implications for glacial-interglacial changes in the ocean silicon cycle. **Paleoceanography**, v. 22, n. 4, p. n/a-n/a, 2007.

BRADTMILLER, L.; MCMANUS, J.; ROBINSON, L. $^{231}Pa/^{230}Th$ evidence for a weakened but persistent Atlantic meridional overturning circulation during Heinrich Stadial 1. **Nature Communications**, v. 5, n. 1, 2014.

BROECKER, W. Glacial to interglacial changes in ocean chemistry. **Progress in Oceanography**, v. 11, n. 2, p. 151-197, 1982.

BROECKER, W. Does the trigger for abrupt climate change reside in the ocean or in the atmosphere? **Science**, v. 300, n. 5625, p. 1519-1522, 2003.

BURCKEL, P. et al. Atlantic Ocean circulation changes preceded millennial tropical South America rainfall events during the last glacial. **Geophysical Research Letters**, v. 42, n. 2, p. 411-418, 2015.

BURCKEL, P. et al. Changes in the geometry and strength of the Atlantic meridional overturning circulation during the last glacial (20–50 ka). **Climate of the Past**, v. 12, n. 11, p. 2061-2075, 2016.

BURKI, F. The eukaryotic tree of life from a global phylogenomic perspective. **Cold Spring Harbor Perspectives in Biology**, v. 6, n. 5, 2014.

CAMACHO, H.; LONGOBUCCO, M. **Los invertebrados fósiles**. Buenos Aires: Fundación de Historia Natural Félix de Azara, 2007.

CHAN, S. et al. Foraminiferal biofacies and depositional environments of the Burdigalian mixed carbonate and siliciclastic Dam Formation, Al-Lidam area, Eastern Province of Saudi Arabia. **Palaeogeography, Palaeoclimatology, Palaeoecology**, v. 469, p. 122-137, 2017.

CHAPMAN, M.; SHACKLETON, N. Millennial-scale fluctuations in North Atlantic heat flux during the last 150,000 years. **Earth and Planetary Science Letters**, v. 159, n. 1-2, p. 57-70, 1998.

CHAPMAN, M.; SHACKLETON, N. Global ice-volume fluctuations, North Atlantic ice-rafting events, and deep-ocean circulation changes between 130 and 70 ka. **Geology**, v. 27, n. 9, p. 795, 1999.

CORLISS, B. Microhabitats of benthic foraminifera within deep-sea sediments. **Nature**, v. 314, n. 6010, p. 435-438, 1985.

CORLISS, B.; CHEN, C. Morphotype patterns of Norwegian Sea deep-sea benthic foraminifera and ecological implications. **Geology**, v. 16, n. 8, p. 716, 1988.

CORLISS, B.; EMERSON, S. Distribution of rose bengal stained deep-sea benthic foraminifera from the Nova Scotian continental margin and Gulf of Maine. **Deep Sea Research Part A. Oceanographic Research Papers**, v. 37, n. 3, p. 381-400, 1990.

CORLISS, B. et al. Influence of seasonal primary productivity on $\delta^{13}C$ of North Atlantic deep-sea benthic foraminifera. **Deep Sea Research Part I: Oceanographic Research Papers**, v. 53, n. 4, p. 740-746, 2006.

CURRY, W.; LOHMANN, G. Reduced advection into Atlantic Ocean deep eastern basins during last glaciation maximum. **Nature**, v. 306, n. 5943, p. 577-580, 1983.

CURRY, W.; OPPO, D. Glacial water mass geometry and the distribution of $\delta^{13}C$ of ΣCO_2 in the western Atlantic Ocean. **Paleoceanography**, v. 20, n. 1, p. n/a-n/a, 2005.

CUSHMAN, J. **Foraminifera. Their classification and economic use**. Sharon: Cushman Laboratory for Foraminiferal Research, 1928. v. 1.

DAUWE, B.; MIDDELBURG, J.; HERMAN, P. Effect of oxygen on the degradability of organic matter in subtidal and intertidal sediments of the North Sea area. **Marine Ecology Progress Series**, v. 215, p. 13-22, 2001.

DENGLER, M. et al. Break-up of the Atlantic deep western boundary current into eddies at 8° S. **Nature**, v. 432, n. 7020, p. 1018-1020, 2004.

DENTON, G. et al. The Last Glacial Termination. **Science**, v. 328, n. 5986, p. 1652-1656, 2010.

DESSANDIER, P. et al. Lateral and vertical distributions of living benthic foraminifera off the Douro River (western Iberian margin): Impact of the organic matter quality. **Marine Micropaleontology**, v. 120, p. 31-45, 2015.

EMERSON, S. et al. Organic carbon dynamics and preservation in deep-sea sediments. **Deep Sea Research Part A. Oceanographic Research Papers**, v. 32, n. 1, p. 1-21, 1985.

ERICSON, D.; WOLLIN, G. Pleistocene climates and chronology in deep-sea sediments. **Science**, v. 162, n. 3859, p. 1227-1234, 1968.

GESLIN, E. et al. Migratory responses of deep-sea benthic foraminifera to variable oxygen conditions: laboratory investigations. **Marine Micropaleontology**, v. 53, n. 3-4, p. 227-243, 2004.

GHERARDI, J. et al. Evidence from the Northeastern Atlantic basin for variability in the rate of the meridional overturning circulation through the last deglaciation. **Earth and Planetary Science Letters**, v. 240, n. 3-4, p. 710-723, 2005.

GIL, I.; KEIGWIN, L.; ABRANTES, F. Deglacial diatom productivity and surface ocean properties over the Bermuda Rise, northeast Sargasso Sea. **Paleoceanography**, v. 24, n. 4, 2009.

GONI, G.; JOHNS, W. A census of North Brazil Current Rings observed from TOPEX/POSEIDON altimetry: 1992-1998. **Geophysical Research Letters**, v. 28, n. 1, p. 1-4, 2001.

GOODAY, A. The biology of deep-sea foraminifera: A review of some advances and their applications in paleoceanography. **PALAIOS**, v. 9, n. 1, p. 14, 1994.

GOTTSCHALK, J. et al. Biological and physical controls in the Southern Ocean on past millennial-scale atmospheric CO_2 changes. **Nature Communications**, v. 7, n. 1, 2016a.

GOTTSCHALK, J. et al. Carbon isotope offsets between benthic foraminifer species of the genus Cibicides (Cibicidoides) in the glacial sub-Antarctic Atlantic. **Paleoceanography**, v. 31, n. 12, p. 1583-1602, 2016b.

GRÖGER, M.; HENRICH, R.; BICKERT, T. Glacial–interglacial variability in lower North Atlantic deep water: inference from silt grain-size analysis and carbonate preservation in the western equatorial Atlantic. **Marine Geology**, v. 201, n. 4, p. 321-332, 2003.

GROSSMAN, E. Stable isotopes in modern benthic foraminifera; a study of vital effect. **The Journal of Foraminiferal Research**, v. 17, n. 1, p. 48-61, 1987.

HASTENRATH, S.; MERLE, J. Annual cycle of subsurface thermal structure in the tropical Atlantic Ocean. **Journal of Physical Oceanography**, v. 17, n. 9, p. 1518-1538, 1987.

HASTENRATH, S. Exploring the climate problems of Brazil's Nordeste: a review. **Climatic Change**, v. 112, n. 2, p. 243-251, 2011.

HEDGES, J.; KEIL, R. Sedimentary organic matter preservation: an assessment and speculative synthesis. **Marine Chemistry**, v. 49, n. 2-3, p. 81-115, 1995.

HEINRICH, H. Origin and consequences of cyclic ice rafting in the Northeast Atlantic Ocean during the past 130,000 years. **Quaternary Research**, v. 29, n. 02, p. 142-152, 1988.

HEMMING, S. Heinrich events: Massive late Pleistocene detritus layers of the North Atlantic and their global climate imprint. **Reviews of Geophysics**, v. 42, n. 1, 2004.

HENRY, L. et al. North Atlantic Ocean circulation and abrupt climate change during the last glaciation. **Science**, v. 353, n. 6298, p. 470-474, 2016.

HERTZBERG, J. et al. Evidence for a biological pump driver of atmospheric CO_2 rise during Heinrich Stadial 1. **Geophysical Research Letters**, v. 43, n. 23, p. 12242-12251, 2016.

HIRSCHI, J. et al. A monitoring design for the Atlantic meridional overturning circulation. **Geophysical Research Letters**, v. 30, n. 7, 2003.

HOEFS, J. **Stable isotope geochemistry**. Berlin: Springer-Verlag, 2009. 340 p.

HONISCH, B. et al. Atmospheric carbon dioxide concentration across the Mid-Pleistocene Transition. **Science**, v. 324, n. 5934, p. 1551-1554, 2009.

HOOGAKKER, B. et al. Gulf Stream – subtropical gyre properties across two Dansgaard–Oeschger cycles. **Quaternary Science Reviews**, v. 81, p. 105-113, 2013.

HOOGAKKER, B. et al. Glacial–interglacial changes in bottom-water oxygen content on the Portuguese margin. **Nature Geoscience**, v. 8, n. 1, p. 40-43, 2015.

HOOGAKKER, B.; THORNALLEY, D.; BARKER, S. Millennial changes in North Atlantic oxygen concentrations. **Biogeosciences**, v. 13, n. 1, p. 211-221, 2016.

HOWE, J. et al. North Atlantic Deep Water production during the Last Glacial Maximum. **Nature Communications**, v. 7, n. 1, 2016.

HOWE, J. et al. Similar mid-depth Atlantic water mass provenance during the Last Glacial Maximum and Heinrich Stadial 1. **Earth and Planetary Science Letters**, v. 490, p. 51-61, 2018.

JACCARD, S. et al. Covariation of deep Southern Ocean oxygenation and atmospheric CO_2 through the last ice age. **Nature**, v. 530, n. 7589, p. 207-210, 2016.

JAESCHKE, A. et al. Coupling of millennial-scale changes in sea surface temperature and precipitation off northeastern Brazil with high-latitude climate shifts during the last glacial period. **Paleoceanography**, v. 22, n. 4, p. n/a-n/a, 2007.

JOHNS, W. et al. Annual cycle and variability of the North Brazil Current. **Journal of Physical Oceanography**, v. 28, n. 1, p. 103-128, 1998.

JORISSEN, F.; DE STIGTER, H.; WIDMARK, J. A conceptual model explaining benthic foraminiferal microhabitats. **Marine Micropaleontology**, v. 26, n. 1-4, p. 3-15, 1995.

KATZ, M. et al. Traditional and emerging geochemical proxies in foraminifera. **The Journal of Foraminiferal Research**, v. 40, n. 2, p. 165-192, 2010.

KEELING, R.; KÖRTZINGER, A.; GRUBER, N. Ocean deoxygenation in a warming world. **Annual Review of Marine Science**, v. 2, n. 1, p. 199-229, 2010.

KEY, R. et al. A global ocean carbon climatology: Results from Global Data Analysis Project (GLODAP). **Global Biogeochemical Cycles**, v. 18, n. 4, p. n/a-n/a, 2004.

KOHFELD, K. et al. Role of marine biology in glacial-interglacial CO_2 cycles. **Science**, v. 308, n. 5718, p. 74-78, 2005.

KOHO, K.; DE NOOIJER, L.; REICHART, G. Combining benthic foraminiferal ecology and shell Mn/Ca to deconvolve past bottom water oxygenation and paleoproductivity. **Geochimica et Cosmochimica Acta**, v. 165, p. 294-306, 2015.

KROOPNICK, P. The distribution of ^{13}C of ΣCO_2 in the world oceans. **Deep Sea Research Part A. Oceanographic Research Papers**, v. 32, n. 1, p. 57-84, 1985.

LACERRA, M. et al. Carbon storage in the mid-depth Atlantic during millennial-scale climate events. **Paleoceanography**, v. 32, n. 8, p. 780-795, 2017.

LAMBELET, M. et al. Neodymium isotopic composition and concentration in the western North Atlantic Ocean: Results from the GEOTRACES GA02 section. **Geochimica et Cosmochimica Acta**, v. 177, p. 1-29, 2016.

LOEBLICH, A.; TAPPAN, H. Introduction. In: _____. **Foraminiferal genera and their classification**. Boston, MA: Springer US, 1988. p. 1–5.

LUMPKIN, R.; SPEER, K. Global ocean meridional overturning. **Journal of Physical Oceanography**, v. 37, n. 10, p. 2550-2562, 2007.

LUND, D. et al. Southwest Atlantic water mass evolution during the last deglaciation. **Paleoceanography**, v. 30, n. 5, p. 477-494, 2015.

LUX, M.; MERCIER, H.; ARHAN, M. Interhemispheric exchanges of mass and heat in the Atlantic Ocean in January–March 1993. **Deep Sea Research Part I: Oceanographic Research Papers**, v. 48, n. 3, p. 605-638, 2001.

MACKENSEN, A. et al. The $\delta^{13}C$ in benthic foraminiferal tests of Fontbotia wuellerstorfi (Schwager) relative to the $\delta^{13}C$ of dissolved inorganic carbon in Southern Ocean Deep Water: Implications for glacial ocean circulation models. **Paleoceanography**, v. 8, n. 5, p. 587-610, 1993.

MACKENSEN, A. et al. Deep-sea foraminifera in the South Atlantic Ocean: Ecology and assemblage generation. **Micropaleontology**, v. 41, n. 4, p. 342, 1995.

MACKENSEN, A. et al. Microhabitat preferences and stable carbon isotopes of endobenthic foraminifera: clue to quantitative reconstruction of oceanic new production? **Marine Micropaleontology**, v. 40, n. 3, p. 233-258, 2000.

MACKENSEN, A. et al. Microhabitat preferences of live benthic foraminifera and stable carbon isotopes off SW Svalbard in the presence of widespread methane seepage. **Marine Micropaleontology**, v. 132, p. 1-17, 2017.

MARSHAK, S. **Essentials of Geology**. 4th ed. New York: W. W. Norton & Company, 2013. 650 p.

MASLIN, M.; SWANN, G. **Isotopes in Palaeoenvironmental Research**: Isotopes in Marine Sediments. [S.l.]: ed. Springer, 2006. 290 p.

MCCAVE, I.; MANIGHETTI, B.; ROBINSON, S. Sortable silt and fine sediment size/composition slicing: Parameters for palaeocurrent speed and palaeoceanography. **Paleoceanography**, v. 10, n. 3, p. 593-610, 1995.

MCCORKLE, D.; EMERSON, S. The relationship between pore water carbon isotopic composition and bottom water oxygen concentration. **Geochimica et Cosmochimica Acta**, v. 52, n. 5, p. 1169-1178, 1988.

MCCORKLE, D. et al. The influence of microhabitats on the carbon isotopic composition of deep-sea benthic foraminifera. **Paleoceanography**, v. 5, n. 2, p. 161-185, 1990.

MCCORKLE, D.; CORLISS, B.; FARNHAM, C. Vertical distributions and stable isotopic compositions of live (stained) benthic foraminifera from the North Carolina and California continental margins. **Deep Sea Research Part I: Oceanographic Research Papers**, v. 44, n. 6, p. 983-1024, 1997.

MCMANUS, J. et al. Collapse and rapid resumption of Atlantic meridional circulation linked to deglacial climate changes. **Nature**, v. 428, n. 6985, p. 834-837, 2004.

MECKLER, A. et al. Deglacial pulses of deep-ocean silicate into the subtropical North Atlantic Ocean. **Nature**, v. 495, n. 7442, p. 495-498, 2013.

MENVIEL, L. et al. Southern Hemisphere westerlies as a driver of the early deglacial atmospheric CO_2 rise. **Nature Communications**, v. 9, n. 1, 2018.

MOLINA, E. **Micropaleontología:** Foraminíferos planctónicos: Globigenina, 2. ed. Zaragoza: Prensas Universitarias de Zaragoza, 2004. 158 p.

MULITZA, S. et al. Synchronous and proportional deglacial changes in Atlantic meridional overturning and northeast Brazilian precipitation. **Paleoceanography**, v. 32, n. 6, p. 622-633, 2017.

NACE, T. et al. The role of North Brazil Current transport in the paleoclimate of the Brazilian Nordeste margin and paleoceanography of the western tropical Atlantic during the late Quaternary. **Palaeogeography, Palaeoclimatology, Palaeoecology**, v. 415, p. 3-13, 2014.

OPPO, D.; CURRY, W.; MCMANUS, J. What do benthic $\delta^{13}C$ and $\delta^{18}O$ data tell us about Atlantic circulation during Heinrich Stadial 1? **Paleoceanography**, v. 30, n. 4, p. 353-368, 2015.

OPPO, D. et al. Data constraints on glacial Atlantic water mass geometry and properties. **Paleoceanography and Paleoclimatology**, v. 33, n. 9, p. 1013-1034, 2018.

PHLEGER, F.; PARKER, F. **Ecology of foraminifera, northwest Gulf of Mexico, Part II: Foraminifera species**. Memoirs of the Geological Society of America, 1951.

PIOTROWSKI, A. et al. Oscillating glacial northern and southern deep water formation from combined neodymium and carbon isotopes. **Earth and Planetary Science Letters**, v. 272, n. 1-2, p. 394-405, 2008.

PORTILHO-RAMOS, R. et al. Coupling of equatorial Atlantic surface stratification to glacial shifts in the tropical rainbelt. **Scientific Reports**, v. 7, n. 1, 2017.

RAVELO, A.; HILLAIRE-MARCEL, C. (Eds.). **Proxies in Late Cenozoic paleoceanography:** The use of oxygen and carbon isotopes of foraminifera in paleoceanography. Tokyo: Elsevier, 2007. 761 p.

REBOTIM, A. et al. Factors controlling the depth habitat of planktonic foraminifera in the subtropical eastern North Atlantic. **Biogeosciences**, v. 14, n. 4, p. 827-859, 2017.

REID, J. On the total geostrophic circulation of the South Atlantic Ocean: Flow patterns, tracers, and transports. **Progress in Oceanography**, v. 23, n. 3, p. 149-244, 1989.

REIMER, P. et al. IntCal13 and Marine13 radiocarbon age calibration curves 0–50,000 years cal BP. **Radiocarbon**, v. 55, n. 04, p. 1869-1887, 2013.

RHEIN, M.; STRAMMA, L.; SEND, U. The Atlantic Deep Western Boundary Current: Water masses and transports near the equator. **Journal of Geophysical Research**, v. 100, n. C2, p. 2441, 1995.

RUDDIMAN, W. **Earth's Climate:** Past and Future. 2th ed. New York: W. H. Freeman & Company, 2008. 412 p.

SCHIEBEL, R.; HEMLEBEN, C. **Planktic foraminifers in the modern ocean**. Berlin Heidelberg: Springer-Verlag, 2017. 358 p.

SCHLITZER, R. Ocean Data View, 2017. Available in: < odv.awi.de >. Access in: jul. 2018.

SCHMIEDL, G.; MACKENSEN, A. Late Quaternary paleoproductivity and deep water circulation in the eastern South Atlantic Ocean: Evidence from benthic foraminifera. **Palaeogeography, Palaeoclimatology, Palaeoecology**, v. 130, n. 1-4, p. 43-80, 1997.

SCHMITTNER, A. et al. Large fluctuations of dissolved oxygen in the Indian and Pacific oceans during Dansgaard-Oeschger oscillations caused by variations of North Atlantic Deep Water subduction. **Paleoceanography**, v. 22, n. 3, p. n/a-n/a, 2007.

SCHMITTNER, A.; LUND, D. Early deglacial Atlantic overturning decline and its role in atmospheric CO_2 rise inferred from carbon isotopes ($\delta^{13}C$). **Climate of the Past**, v. 11, n. 2, p. 135-152, 2015.

SCHOTT, F.; STRAMMA, L.; FISCHER, J. The warm water inflow into the western tropical Atlantic boundary regime, spring 1994. **Journal of Geophysical Research**, v. 100, n. C12, p. 24745, 1995.

SCHOTT, F. et al. The zonal currents and transports at 35°W in the tropical Atlantic. **Geophysical Research Letters**, v. 30, n. 7, 2003.

SEN GUPTA, B.; MACHAIN-CASTILLO, M. Benthic foraminifera in oxygen-poor habitats. **Marine Micropaleontology**, v. 20, n. 3-4, p. 183-201, 1993.

SEN GUPTA, B. (Ed.). **Modern Foraminifera**. Boston: Kluwer Academic Publishers, 2003. 371 p.

SIGMAN, D.; BOYLE, E. Glacial/interglacial variations in atmospheric carbon dioxide. **Nature**, v. 407, n. 6806, p. 859-869, 2000.

SPERO, H. et al. Effect of seawater carbonate concentration on foraminiferal carbon and oxygen isotopes. **Nature**, v. 390, n. 6659, p. 497-500, 1997.

STRAMMA, L.; FISCHER, J.; REPPIN, J. The North Brazil Undercurrent. **Deep Sea Research Part I: Oceanographic Research Papers**, v. 42, n. 5, p. 773-795, 1995.

STRAMMA, L.; ENGLAND, M. On the water masses and mean circulation of the South Atlantic Ocean. **Journal of Geophysical Research: Oceans**, v. 104, n. C9, p. 20863-20883, 1999.

STREETER, S. Bottom water and benthonic foraminifera in the North Atlantic – Glacial-interglacial contrasts. **Quaternary Research**, v. 3, n. 01, p. 131-141, 1973.

SZCZYGIELSKI, A. et al. Evolution of the Parnaíba Delta (NE Brazil) during the late Holocene. **Geo-Marine Letters**, v. 35, n. 2, p. 105-117, 2014.

TACHIKAWA, K.; ELDERFIELD, H. Microhabitat effects on Cd/Ca and $\delta^{13}C$ of benthic foraminifera. **Earth and Planetary Science Letters**, v. 202, n. 3-4, p. 607-624, 2002.

THEODOR, M. et al. Stable carbon isotope gradients in benthic foraminifera as proxy for organic carbon fluxes in the Mediterranean Sea. **Biogeosciences**, v. 13, n. 23, p. 6385-6404, 2016.

THOMPSON, L.; DANABASOGLU, G.; PATTERSON, M. Observing and Modeling the Atlantic Meridional Overturning Circulation. **Eos**, v. 96, 2015.

TOGGWEILER, J.; RUSSELL, J.; CARSON, S. Midlatitude westerlies, atmospheric CO_2, and climate change during the ice ages. **Paleoceanography**, v. 21, n. 2, p. n/a-n/a, 2006.

UFKES, E.; FRED JANSEN, J.; BRUMMER, G. Living planktonic foraminifera in the eastern South Atlantic during spring: Indicators of water masses, upwelling and the Congo (Zaire) River plume. **Marine Micropaleontology**, v. 33, n. 1-2, p. 27-53, 1998.

VAN DER ZWAAN, G. Paleoecology of late Miocene Mediterranean foraminifera. **Utrecht Micropaleontogical Bulletin**, v. 25, p. 1-205, 1982.

VENANCIO, I. et al. Millennial- to orbital-scale responses of western equatorial Atlantic thermocline depth to changes in the trade wind system since the Last Interglacial. **Paleoceanography and Paleoclimatology**, v. 33, n. 12, p. 1490-1507, 2018.

VENTURELLI, R. et al. Epifaunal foraminifera in an infaunal world: Insights into the influence of heterogeneity on the benthic ecology of oxygen-poor, deep-sea habitats. **Frontiers in Marine Science**, v. 5, 2018.

VINK, A. et al. Shifts in the position of the north equatorial current and rapid productivity changes in the western tropical Atlantic during the last glacial. **Paleoceanography**, v. 16, n. 5, p. 479-490, 2001.

VOIGT, I. et al. Variability in mid-depth ventilation of the western Atlantic Ocean during the last deglaciation. **Paleoceanography**, v. 32, n. 9, p. 948-965, 2017.

WAELBROECK, C. et al. Relative timing of precipitation and ocean circulation changes in the western equatorial Atlantic over the last 45kyr. **Climate of the Past**, v. 14, n. 9, p. 1315-1330, 2018.

WANG, P.; TIAN, J.; LOURENS, L. Obscuring of long eccentricity cyclicity in Pleistocene oceanic carbon isotope records. **Earth and Planetary Science Letters**, v. 290, n. 3-4, p. 319-330, 2010.

WOLFF, E. et al. Millennial-scale variability during the last glacial: The ice core record. **Quaternary Science Reviews**, v. 29, n. 21-22, p. 2828-2838, 2010.

WOODRUFF, F.; SAVIN, S.; DOUGLAS, R. Biological fractionation of oxygen and carbon isotopes by recent benthic foraminifera. **Marine Micropaleontology**, v. 5, p. 3-11, 1980.

ZAHN, R.; WINN, K.; SARNTHEIN, M. Benthic foraminiferal $\delta^{13}C$ and accumulation rates of organic carbon: Uvigerina peregrina group and Cibicidoides wuellerstorfi. **Paleoceanography**, v. 1, n. 1, p. 27-42, 1986.

ZHANG, Y. et al. Origin of increased terrigenous supply to the NE South American continental margin during Heinrich Stadial 1 and the Younger Dryas. **Earth and Planetary Science Letters**, v. 432, p. 493-500, 2015.

APPENDIX – SPECIES REFERENCE LIST

The following is a list of the benthic and planktonic foraminifera species identified in this study.

Cibicides wuellerstorfi Schwager, 1866.

Globigerina bulloides d'Orbigny, 1826.

Globobulimina affinis d'Orbigny, 1839.

Neogloboquadrina dutertrei d'Orbigny, 1839.

Neogloboquadrina incompta Cifelli, 1961.

Uvigerina peregrina Cushman, 1923.

ANNEX I – TABLE OF TOTAL ORGANIC CARBON (TOC) AND SORTABLE SILT ($\overline{SS}$) GRAIN-SIZE FRACTION FROM CORE GL-1248

Depth (cm)	Age (kyr)	TOC (%)	$\overline{SS}$ (µm)
220	29,09	0,83	11,40
224	29,15	0,85	11,89
230	29,24	0,88	11,85
234	29,30	0,74	12,62
240	29,39	0,86	11,76
244	29,45	0,86	11,50
250	29,54	0,84	11,86
254	29,60	0,88	12,60
260	29,69	0,82	11,63
264	29,75		11,83
270	29,84	0,73	11,88
274	29,90	0,74	12,33
280	29,99	0,70	11,71
284	30,05	0,66	12,47
290	30,14	0,74	11,86
294	30,20	0,77	12,70
300	30,29	0,69	12,69
304	30,35	0,74	12,70
310	30,44	0,96	11,92
320	30,59	0,69	13,11
324	30,65	0,69	13,08
330	30,74	0,74	11,82
334	30,80	0,79	12,41
340	30,94	0,80	12,81
344	31,09	0,78	13,01
350	31,31	0,77	12,39
354	31,46	0,85	12,40
360	31,69	0,87	13,08
364	31,84	0,77	13,54
380	32,44	0,74	11,40
384	32,59	0,81	11,89
390	32,95	0,78	12,46
394	33,24	0,85	13,20
404	33,95	0,88	12,98
410	34,38	0,95	12,84
414	34,66	0,83	13,17
420	34,89	0,81	12,79
424	35,04	0,84	11,89

430	35,26	0,78	12,49
434	35,41	0,81	12,50
440	35,63	0,96	13,27
444	35,78	0,74	13,23
450	36,02	0,56	12,75
454	36,19	0,86	11,92
460	36,43	1,05	13,17
464	36,60	0,98	13,41
470	36,84	1,04	13,33
474	37,01	0,84	12,97
480	37,25	0,83	13,49
484	37,42	0,72	13,43
490	37,66	0,77	13,20
494	37,83	0,67	13,12
498	37,99	0,72	12,52
504	38,24	0,82	11,66
510	38,37	1,04	11,82
514	38,45	0,96	11,45
520	38,58	0,98	11,89
524	38,67	1,15	11,84
530	38,80	0,97	10,93
534	38,88	0,99	11,80
540	39,01	0,95	11,54
544	39,10	1,00	11,28
550	39,23	0,93	11,78
554	39,47	0,75	11,60
560	39,83	0,82	12,95
564	40,07	0,77	12,84
570	40,43	0,74	13,16
574	40,67	0,72	11,91
580	41,03	0,86	13,08
584	41,27	0,88	13,17
590	41,63	0,84	13,08
594	41,87	0,71	13,04
600	42,23	0,74	10,85
604	42,47	0,60	11,66
610	42,83	0,72	11,55
614	43,07	0,72	13,11
620	43,43	0,78	11,55
624	43,67	0,71	11,36
630	44,04	0,76	11,76
638	44,27	0,89	13,04
644	44,45	0,84	13,47

650	44,62	0,67	12,97
654	44,74	0,79	13,43
660	44,92	0,80	13,18
664	45,04	0,78	12,84
670	45,21	0,86	13,58
674	45,33	0,77	13,06
680	45,51	0,77	13,53
684	45,62	0,72	13,97
694	45,92	0,80	10,57
698	46,04	0,70	11,67
710	46,39	0,66	12,60
714	46,51	0,59	13,09
720	46,68	0,69	11,83
724	46,80	0,64	12,83
730	47,00	0,97	11,41
734	47,14	0,97	11,83
740	47,35	0,89	10,56
744	47,50	0,90	11,51
750	47,71	0,92	11,37
754	47,85	0,85	10,78
764	48,20	0,88	11,37
770	48,42	0,84	10,76
774	48,56	0,94	11,90
780	48,77	0,81	10,89
784	48,94	0,65	12,61
790	49,24	0,75	11,76
794	49,44	0,84	11,62
804	49,94	0,62	10,82
814	50,44	0,78	11,73
820	50,74	0,72	11,71
826	51,04	0,84	11,61
830	51,24	0,85	11,55
834	51,44	0,96	11,58
840	51,73	0,74	11,89
844	51,93	0,79	12,52
850	52,23	0,75	11,85
854	52,43	0,78	12,33
860	52,73	0,75	11,90
864	52,93	0,75	12,74
870	53,23	0,81	14,77
874	53,43	0,89	12,70
880	53,73	0,77	12,57
884	53,93	0,89	11,90

890	54,23	0,77	12,54
900	54,73	0,64	13,41
904	54,87	0,85	11,62
908	55,00	0,78	10,93
914	55,18	0,86	
920	55,37	0,72	12,46
924	55,49	0,67	13,06
930	55,68	0,82	12,98
934	55,83	0,75	12,69
940	56,12	0,84	13,59
944	56,30	0,69	13,83
950	56,59	0,81	14,54
954	56,78	0,79	13,28
960	57,06	0,80	13,37
964	57,25	0,87	13,48
970	57,53	0,85	12,62
974	57,72	0,77	12,21
980	58,00	0,77	12,37
984	58,19	0,68	12,56
990	58,47	0,59	12,38
994	58,66	0,64	12,43
1000	58,94	0,64	11,68
1004	59,13	0,69	12,59
1010	59,56	0,98	12,15
1014	60,05	0,92	12,78
1020	60,77	0,87	12,53
1024	61,26	0,93	12,30
1030	61,98	0,87	11,86

Source: Elaborated by the author, 2019.

ANNEX II – TABLE OF STABLE CARBON ISOTOPES ($\delta^{13}C$), GRADIENT BETWEEN STABLE CARBON ISOTOPES ($\Delta\delta^{13}C$) AND RECONSTRUCTION OF BOTTOM-WATER OXYGENATION ($[O_2]$) FROM CORE GL-1248

Depth (cm)	Age (kyr)	$\delta^{13}C$ C.wu (‰)	$\delta^{13}C$ U.pe (‰)	$\delta^{13}C$ G.af (‰)	$\Delta\delta^{13}C_{U.pe-C.wu}$ (‰)	$\Delta\delta^{13}C_{C.wu-G.af}$ (‰)	$[O_2]$ ($\mu mol.kg^{-1}$)
226	29,18		-1,08				
230	29,24		-0,41				
234	29,30		-1,12				
236	29,33		-1,01				
238	29,36		-1,29				
242	29,42	0,36	**-0,04**	-2,28	-0,40	2,64	288,28
244	29,45		-0,46				
262	29,72	0,86		-2,21		3,07	344,37
264	29,75	1,09	-0,02		-1,11		
278	29,96	0,69		-2,27		2,96	330,12
280	29,99	0,69		-2,26		2,95	328,57
282	30,02	-0,21					
296	30,23	0,81		-1,95		2,76	303,18
298	30,26	0,63		-2,29		2,92	323,90
302	30,32	0,32		-1,96		2,28	241,00
306	30,38	0,67		-2,04		2,70	296,57
310	30,44	0,65		-1,99		2,63	287,51
314	30,50	**0,70**	-0,12	-1,77	-0,83	2,48	267,17
324	30,65	0,85	**-0,15**	-2,41	-1,00	3,26	368,85
330	30,74	1,60		-1,88		3,48	396,57
332	30,77	**1,49**	-0,18		-1,67		
338	30,86	**1,15**	-0,46		-1,61		
346	31,16	0,71	-0,60	**-2,18**	-1,30	2,89	320,41
348	31,24	0,66	**-0,67**	-2,22	-1,33	2,88	319,50
354	31,46	0,81		-2,14		2,95	328,96
358	31,61	0,88	**-1,00**	-2,21	-1,88	3,09	346,44
362	31,76		-0,34				
374	32,22	0,66	-1,47	**-2,15**	-2,13	2,81	310,43
398	33,52	0,54		-2,12		2,66	290,48
404	33,95	1,12		-1,96		3,08	344,76
414	34,66	1,10		-1,93		3,03	338,80
418	34,81	1,06		-1,86		2,91	323,77
422	34,96	0,53	-0,21	-2,46	-0,75	2,99	333,36
426	35,11	0,61	-0,79	-2,19	-1,39	2,80	308,75
434	35,41	**0,60**	-0,68		-1,28		
446	35,86	0,58		-2,36		2,94	327,53

454	36,19	0,64		-2,06		2,71	296,70
456	36,27	0,71		-2,15		2,85	315,61
458	36,35	0,84	-0,86	-2,17	-1,70	3,02	336,86
460	36,43	0,83		-2,00		2,82	312,12
462	36,51	0,85	**-0,80**	-2,06	-1,65	2,92	323,90
470	36,84	0,77	**-0,68**	-2,81	-1,45	3,58	409,91
474	37,01	0,58		-2,09		2,66	291,13
478	37,17	**0,69**	-0,57	-2,48	-1,25		
482	37,34	0,80		-2,33		3,13	352,27
484	37,42	0,79	**-0,50**	-2,45	-1,29	3,24	366,00
490	37,66	0,62		**-2,61**		3,23	364,45
494	37,83	1,06	-0,40	-2,71	-1,45	3,77	434,53
498	37,99	0,88	**-0,50**	-1,98	-1,38	2,86	316,26
504	38,24		-0,67				
506	38,28		-1,08				
514	38,45		-0,67				
528	38,75	0,20	**-0,47**	-2,13	-0,67	2,32	247,22
536	38,93	**0,32**	-0,36		-0,68		
538	38,97	**0,36**	-0,48		-0,84		
554	39,47	0,62	**-0,24**	-2,25	-0,85	2,86	317,04
556	39,59		-0,21				
574	40,67	**0,71**	-0,99	-2,32	-1,70	3,03	343,98
580	41,03	0,62		-2,15		2,77	305,64
584	41,27	0,90		-2,31		3,20	361,34
586	41,39	0,90		-2,12		3,02	338,02
590	41,63	0,73		-2,22		2,95	328,96
594	41,87	0,93		-2,33		3,26	368,08
598	42,11	1,04		-2,17		3,21	361,99
600	42,23	0,96		-2,39		3,36	381,03
602	42,35	0,87		-2,44		3,31	375,33
606	42,59	0,94		-2,00		2,93	326,37
618	43,31	1,02		-1,87		2,89	320,54
622	43,55	0,70		-2,22		2,92	324,94
626	43,80	1,02		-2,11		3,13	351,37
630	44,04	0,92		-2,30		3,22	363,54
638	44,27	0,87		-2,77		3,64	417,17
640	44,33	0,84		-2,47		3,31	374,68
648	44,56	0,93		-2,45		3,38	384,01
650	44,62		-0,78				
654	44,74	0,86	**-0,81**	-2,59	-1,67	3,45	393,20
656	44,80		-0,82				
666	45,09	0,74	**-0,42**	-2,35	-1,16	3,09	346,96
670	45,21	0,74	-0,26	-2,16	-1,00	2,89	320,80

672	45,27	0,76		**-2,23**		2,99	333,62
676	45,39	0,88		-2,38		3,26	368,98
678	45,45	1,09		-2,63		3,72	428,31
682	45,57	0,61		-2,59		3,20	360,17
686	45,68	1,06		-2,36		3,42	389,71
690	45,80	0,94		-2,40		3,34	378,83
694	45,92	1,18	-0,39	-2,21	-1,57	3,39	385,43
698	46,04	1,18	**-0,28**	-2,56	-1,46	3,74	400,85
702	46,15	1,04	-0,17	-2,35	-1,21	3,39	384,91
706	46,27	0,98	**-0,15**	-2,68	-1,12	3,65	419,37
710	46,39	1,15	-0,23	-2,68	-1,38	3,83	442,56
718	46,62	1,07		**-2,51**		3,58	409,66
724	46,80	1,10		-2,38		3,48	396,96
730	47,00	1,20		**-2,54**		3,74	430,64
734	47,14	0,54		-2,65		3,19	359,78
736	47,21	1,00					
740	47,35	0,71	**-0,59**	**-2,60**	-1,30	3,31	375,59
760	48,06		-1,05				
774	48,56		-1,17				
776	48,63		-0,94				
780	48,77	0,59	**-0,85**	-2,12	-1,44	2,71	297,09
782	48,84	1,09		-2,12		3,21	361,73
786	49,04	0,60	-0,71	-1,90	-1,31	2,50	269,63
794	49,44	0,91		-1,88		2,79	307,71
798	49,64	0,97	**-0,94**	-2,08	-1,91	3,05	341,00
802	49,84	1,09		-2,06		3,00	354,09
804	49,94	0,94	-1,06	-2,22	-2,00	3,15	354,73
808	50,14	0,80		-2,34		3,15	354,09
814	50,44	1,06		-2,42		3,48	397,35
818	50,64	1,01		-2,06		3,07	343,98
822	50,84	1,07		-2,10		3,18	357,84
828	51,14	0,99		-2,06		3,05	340,87
832	51,34	0,90		**-2,20**		3,10	347,22
834	51,44	0,18	-0,20	-2,27	-0,38	2,44	262,76
836	51,53	**0,52**		-2,32		2,84	314,58
840	51,73	1,03	**-0,10**	**-2,34**	-1,13	3,37	382,45
842	51,83	1,02	-0,60	-2,35	-1,62	3,36	381,68
846	52,03	0,99	**-0,54**	-2,24	-1,54	3,24	365,35
850	52,23	1,07		**-2,34**		3,41	387,51
858	52,63	0,88		-2,54		3,42	389,84
862	52,83	1,00	-0,38	-2,26	-1,37	3,26	368,46
866	53,03	1,12	-0,09	-2,37	-1,21	3,49	398,77
870	53,23	1,15		-2,20		3,35	380,77

874	53,43	1,28	**-0,22**		-1,50		
878	53,63	**1,16**		-1,73		2,89	320,54
886	54,03	0,92	**-0,42**	-2,40	-1,33	3,45	393,33
890	54,23		-0,48				
900	54,73	0,93	**-1,12**	-2,48	-2,04	3,41	387,63
902	54,81	**0,98**		-2,38		3,36	381,42
906	54,93	1,08		-2,80		3,88	449,16
910	55,06	**0,94**	-1,76	-2,69		3,63	416,26
914	55,18	**0,72**	-0,88	-2,91	-1,60		
918	55,31	0,65		**-2,71**		3,36	381,42
924	55,49	0,72		**-2,40**		3,12	350,07
928	55,62	0,69		**-2,19**		2,89	320,28
930	55,68	**0,80**		-2,09		2,89	320,80
934	55,83	1,02		-2,40		3,42	389,06
936	55,93	0,82		-2,61		3,44	391,52
938	56,02			-2,40			
942	56,21	0,93		**-2,36**		3,29	372,35
946	56,40	**0,90**	-0,52	-2,31	-1,42		
950	56,59	**0,88**		-2,21		3,09	346,83
954	56,78	**0,87**		-2,14		3,01	335,69
958	56,96	**0,83**	-0,92	-2,08	-1,75		
962	57,15	**0,83**		-2,12		2,95	328,83
966	57,34	0,81		-2,18		2,99	333,36
970	57,53	0,84		-2,54		3,38	384,40
974	57,72	0,70		-2,49		3,19	359,40
978	57,91	0,79		-2,87		3,66	420,28
980	58,00	0,64		**-2,89**		3,53	403,05
982	58,09			-2,92			
986	58,28	**0,71**		-2,94		3,65	418,98
988	58,38	0,76					
990	58,47	0,53	-0,72		-1,25		
992	58,57	0,79	**-0,60**	**-3,00**	-1,39	3,29	371,83
996	58,75		-0,36				
998	58,85	0,79	-0,44	**-3,01**	-1,23	3,80	438,67
1000	58,94	0,36	-0,45	**-3,10**	-0,82	3,46	394,89
1002	59,04	0,77	-0,71		-1,48		
1006	59,23			-3,17			
1010	59,56			-3,03			

Source: Elaborated by the author, 2019.

Note 1: C.wu stands for *C. wuellerstorfi*, U.pe stands for *U. peregrina* and G.af stands for *G. affinis*.
Note 2: Values in bold indicate interpolated data.

ANNEX III – TABLE OF PLANKTONIC FORAMINIFERA PRODUCTIVITY SPECIES FROM CORE GL-1248

Depth (cm)	Age (kyr)	Productivity species (%)
222	29,12	8,05
230	29,24	10,90
242	29,42	9,22
250	29,54	5,69
262	29,72	12,22
274	29,90	18,55
282	30,02	17,60
290	30,14	17,29
302	30,32	23,12
310	30,44	24,47
322	30,62	20,56
330	30,74	19,06
342	31,01	11,35
350	31,31	22,55
362	31,76	20,86
370	32,06	16,86
382	32,52	16,01
390	32,95	23,88
402	33,81	26,27
410	34,38	26,60
422	34,96	22,61
430	35,26	17,91
440	35,63	16,95
450	36,02	31,85
460	36,43	27,73
470	36,84	27,05
480	37,25	25,94
490	37,66	24,77
502	38,16	18,70
510	38,37	18,93
520	38,58	13,53
530	38,80	15,75
540	39,01	14,28
550	39,23	19,26
560	39,83	19,30
570	40,43	21,37
582	41,15	23,02

590	41,63	23,09
600	42,23	18,16
610	42,83	17,52
620	43,43	19,14
630	44,04	25,59
640	44,33	19,35
652	44,68	13,51
660	44,92	13,67
672	45,27	17,23
680	45,51	29,85
690	45,80	26,82
700	46,09	20,38
710	46,39	18,19
720	46,68	13,93
730	47,00	10,74
742	47,43	14,10
752	47,78	18,25
762	48,13	15,44
772	48,49	14,75
780	48,77	15,46
792	49,34	21,45
800	49,74	19,29
812	50,34	17,88
820	50,74	21,15
830	51,24	16,14
842	51,83	15,50
850	52,23	11,64
860	52,73	16,90
870	53,23	15,49
880	53,73	13,69
890	54,23	16,17
900	54,73	12,12
910	55,06	9,11
920	55,37	12,77
930	55,68	12,06
940	56,12	17,62
950	56,59	18,60
960	57,06	24,70
970	57,53	18,73
982	58,09	11,72
990	58,47	19,44
1000	58,94	14,37
1010	59,56	13,83

1020	60,77	12,73
1030	61,98	11,51
1040	63,19	10,89
1050	64,40	8,96

Source: Elaborated by the author, 2019.